⌘ *Author's Choice*

THE JOURNAL OF BIOLOGICAL CHEMISTRY VOL. 287, NO. 35, pp. 29362–29372, August 24, 2012

Cell Surface Expression of the Major Amyloid-β Peptide (Aβ)-degrading Enzyme, Neprilysin, Depends on Phosphorylation by Mitogen-activated Protein Kinase/Extracellular Signal-regulated Kinase Kinase (MEK) and Dephosphorylation by Protein Phosphatase 1a*[S]

Received for publication, January 6, 2012, and in revised form, June 27, 2012 Published, JBC Papers in Press, July 5, 2012, DOI 10.1074/jbc.M112.340372

Naomasa Kakiya[‡§1], Takashi Saito[‡1], Per Nilsson[‡], Yukio Matsuba[‡], Satoshi Tsubuki[‡], Nobuyuki Takei[§], Hiroyuki Nawa[§], and Takaomi C. Saido[‡2]

From the [‡]Laboratory for Proteolytic Neuroscience, RIKEN Brain Science Institute, 2-1 Hirosawa, Wako-shi, Saitama 351-0198, Japan and the [§]Department of Molecular Neurobiology, Brain Research Institute, Niigata University, Niigata 951-8585, Japan

Background: Neprilysin is a major Aβ-degrading enzyme, the expression of which is reduced in the AD brain.
Results: The phosphorylation status of the neprilysin intracellular domain regulates localization and cell surface activity.
Conclusion: Regulation of neprilysin through phosphorylation influences Aβ levels.
Significance: Our results indicate that neprilysin phosphorylation/dephosporylation could be one druggable target in the development of an AD-modifying treatment.

Neprilysin is one of the major amyloid-β peptide (Aβ)-degrading enzymes, the expression of which declines in the brain during aging. The decrease in neprilysin leads to a metabolic Aβ imbalance, which can induce the amyloidosis underlying Alzheimer disease. Pharmacological activation of neprilysin during aging therefore represents a potential strategy to prevent the development of Alzheimer disease. However, the regulatory mechanisms mediating neprilysin activity in the brain remain unclear. To address this issue, we screened for pharmacological regulators of neprilysin activity and found that the neurotrophic factors brain-derived neurotrophic factor, nerve growth factor, and neurotrophins 3 and 4 reduce cell surface neprilysin activity. This decrease was mediated by MEK/ERK signaling, which enhanced phosphorylation at serine 6 in the neprilysin intracellular domain (S6-NEP-ICD). Increased phosphorylation of S6-NEP-ICD in primary neurons reduced the levels of cell surface neprilysin and led to a subsequent increase in extracellular Aβ levels. Furthermore, a specific inhibitor of protein phosphatase-1a, tautomycetin, induced extensive phosphorylation of the S6-NEP-ICD, resulting in reduced cell surface neprilysin activity. In contrast, activation of protein phosphatase-1a increased cell surface neprilysin activity and lowered Aβ levels. Taken together, these results indicate that the phosphorylation status of S6-NEP-ICD influences the localization of neprilysin and affects extracellular Aβ levels. Therefore, maintaining S6-NEP-ICD in a dephosphorylated state, either by inhibition of protein kinases involved in its phosphorylation or by activation of phosphatases catalyzing its dephosphorylation, may represent a new approach to prevent reduction of cell surface neprilysin activity during aging and to maintain physiological levels of Aβ in the brain.

Impaired metabolism of amyloid β peptide (Aβ)[3] in the brain is likely to play a central role in the pathogenesis of Alzheimer disease (AD) (1). Genetically, causative genes in familial AD link mutations in amyloid precursor protein (APP) and presenilins to aberrant increased generation of Aβ42 and Aβ43, the 42- and 43-mer forms of Aβ, respectively. Aβ42 and Aβ43 have higher amyloidogenecity and neural toxicity than Aβ40 (1–4) and lead to the early onset of AD. However, Aβ amyloidosis in sporadic AD, which comprises over 90% of all AD cases, may be caused by a decline in Aβ degradation, Aβ clearance, or both (5). We previously identified neprilysin as a major physiological Aβ-degrading enzyme that regulates the steady-state levels of Aβ species in the brain (6, 7). Consistent with the increase in Aβ levels observed during aging and in AD, the expression levels of neprilysin in the brain decrease with age and in the early stages of AD (8–12). Genetic ablation of neprilysin not only markedly accelerates amyloid plaque formation but also leads to increased impairment of synaptic plasticity and memory formation in APP transgenic mice (13, 14). In contrast, elevation of neprilysin expression/activity promotes Aβ degradation and reduces the accumulation of both soluble and fibrillary Aβ in APP transgenic mice (15–17). Based on these observations, we previously searched for factors that could increase neprilysin activity pharmacologically, identifying somatostatin as a nepri-

* This study was supported by research grants from RIKEN Brain Science Institute; the Ministry of Education, Culture, Sports, Science, and Technology; and the Ministry of Health, Labor, and Welfare of Japan. This study was also supported by the Junior Research Associate Program of RIKEN.
⌘ *Author's Choice*—Final version full access.
[S] This article contains supplemental Figs. S1–S6.
[1] Both authors contributed equally to this work.
[2] To whom correspondence should be addressed. Tel.: 81-48-467-9715; Fax: 81-48-467-9716; E-mail: saido@brain.riken.jp.

[3] The abbreviations used are: Aβ, amyloid β peptide; AD, Alzheimer disease; APP, amyloid precursor protein; BDNF, brain-derived neurotrophic factor; CTF, C-terminal fragment of APP; ICD, intracellular domain; NEP, neprilysin; hNEP, human NEP; NT, neurotrophin; PP1 and PP2, protein phosphatase-1 and -2, respectively; SFV, Semliki Forest virus; MCA, methyl cumaryl amide.

lysin up-regulator, although the underlining mechanisms remain unclear (18).

In this study, we investigated the effect of the neurotrophic factors brain-derived neurotrophic factor (BDNF), nerve growth factor (NGF), and neurotrophins 3 and 4 (NT-3 and -4) and found that they cause a reduction in cell surface neprilysin activity through MAPK signaling. Moreover, our results reveal that cell surface neprilysin activity and localization are regulated by phosphorylation and dephosphorylation at the neprilysin intracellular domain, with a reduction in neprilysin activity leading to an increase in Aβ levels. We therefore speculate that possible drug targets involving neprilysin could include factors involved in the phosphorylation/dephosphorylation of this Aβ-lowering enzyme.

EXPERIMENTAL PROCEDURES

Materials—The reagents used in this study were purchased as follows: BDNF, NGF, NT-3, NT-4, cyclosporin A, and FK-506 (Sigma); U0126 (Enzo Life Sciences); fostriecin, okadic acid, and tautomycetin (Calbiochem); and recombinant human neprilysin (R&D Systems). The phospho-human neprilysin antibodies pS4-NEP, pS6-NEP, pT11-NEP, pT15-NEP, and pT25-NEP were obtained by immunizing rabbits with the following respective synthetic peptides containing phosphoserine (pS) or phosphothreonine (pT) residues: GKpSESQMC, GKSEpSQC, QMDIpTDINTC, TDINpTPKPKC, and KQRWpTPLEC (19, 20). The specificities of the purified phospho-antibodies were investigated by dot blot analysis (21) (see supplemental Fig. S3).

Cell Culture—Human SH-SY5Y neuroblastoma cells were obtained from the European Collection of Cell Cultures. Cells were cultured in 5% CO_2 at 37 °C, as previously described (22). The medium comprised a 1:1 mixture of minimum essential medium and Ham's F-12 medium (Nacalai Tesque), supplemented with 1 μM non-essential amino acids, 100 units/ml penicillin, 100 mg/ml streptomycin, and 15% fetal bovine serum (Invitrogen). Primary cortical/hippocampal neurons derived from wild-type or neprilysin-deficient mouse embryos were isolated as described previously (18). The neurons were plated at 5.0×10^4 cells/well in 96-well plates, 2.0×10^5 cells on glass coverslips (Hamanami) placed in 24-well plates, or 1.0×10^6 cells/well in 6-well plates. After 14 days *in vitro*, primary neurons were subjected to the various assays.

Mutagenesis and Transfection—S4A-, S6A-, T11A-, T15A- and T25A-human neprilysin mutants were generated using a KOD-Plus mutagenesis kit (Toyobo) according to the manufacturer's protocol. To introduce the mutations into human neprilysin cDNA previously cloned into pcDNA3.1 (23), the following primer sets were designed: S4A, 5′-GCAGAAAGTCAGATGGATATA-3′ and 5′-CTTGCCCATCACCTAGGCTGC-3′; S6A, 5′-GCTCAGATGGATATAACTGATATC-3′ and 5′-TTCTGACTTGCCCATCACCTAGG-3′; T11A, 5′-GCTGATATCAACACTCCAAAGC-3′ and 5′-TATATCCATCTGACTTTCTG-3′; T15A, 5′-GCTCCAAAGCCAAAGAAGAAACAGC-3′ and 5′-GTTGATATCAGTTATATCCATCTG-3′; and T25A, 5′-GGCTCCACTGGAGATCAGCCTCTCG-3′ and 5′-CATCGCTGTTTCTTCTTTGGCTTTG-3′ (underlined, original T, AG, A, A, and A, respectively). Constitutive active protein phosphatase-1a (PP1a)-T320A (24) was generated using the KOD-Plus mutagenesis kit, using the following primer set: 5′-GCCCCACCCCGCAATTCCGCCAAA-3′ and 5′-GATGGGTCGGCCTCCAGGGTTCAG-3′ (underlined, original A to G mutation). The mutant genes were transfected into SH-SY5Y cells using FuGENE transfection reagent (Roche Applied Science) according to the manufacturer's instructions. Cells were harvested with lysis buffer containing 0.1 M Tris-HCl, pH 7.5, EDTA-free complete protease inhibitor mixture (Roche Applied Science), 1% Triton X-100, 0.15 M NaCl, 1 mM Na_3VO_4, 1 mM NaF, and 1 μg/ml pepstatin A (Peptide Institute) 48–72 h after transfection.

Cell Surface and Whole-cell Neprilysin Activity—Activity staining of neprilysin using primary neurons was performed as described previously (18), with slight modifications. Because the endogenous neprilysin activity was too low in the primary neurons and SH-SY5Y cells, the cells were infected with Semliki Forest virus containing human neprilysin cDNA (SFV-hNEP), as previously described (25). Twenty-four h postinfection at day *in vitro* 14, neurotrophic factors or other reagents were added, and the cells were incubated for 24 h. They were then fixed with 1.5% paraformaldehyde in 50 mM phosphate buffer (pH 6.8) for 5 min at room temperature. The fixed neurons were incubated in substrate solution (0.25 mM glutaryl-Ala-Ala-Phe-methoxy-2-naphthylamide in 50 mM Tris-HCl, pH 7.4) at 37 °C for 2 h. Leucine aminopeptidase (Sigma), phosphoramidon (Peptide Institute), and nitrosalicylaldehyde (Sigma-Aldrich) were then added to the substrate solution at a final concentration of 50 μg/mg, 10 μM, and 0.6 mM, respectively, and incubated for 30 min at 37 °C. Quantification of the fluorescence signal arising from cell surface neprilysin activity was performed as described previously (18). Cell surface and whole-cell neprilysin activity of SH-SY5Y cells expressing mutant neprilysin were measured as described previously (26), with slight modifications (supplemental Fig. S5). Before the addition of neurotrophic factors, the cells were starved for 48 h to eliminate the effect of serum. After a 24-h treatment with neurotrophic factors, cells or lysates were incubated with substrate mixture (50 μM suc-Ala-Ala-Phe-MCA (Peptide Institute) and 10 nM benzyloxycarbonyl (Z)-Leu-Leu-Leucinal in 50 mM MES, pH 6.5, with or without 10 μM thiorphan (neprilysin-specific inhibitor)) at 37 °C for 30 min. Following this, 0.1 mg/ml leucine aminopeptidase (Sigma) and 0.1 mM phosphoramidon were added, and the reaction mixture was incubated at 37 °C for a further 30 min. 7-Amino-4-methylcoumarin fluorescence was measured at excitation and emission wavelengths of 380 and 460 nm, respectively. After measurement, cells were collected and subjected to Western blot analysis to evaluate neprilysin levels.

Cell Surface Biotinylation—The cell membrane of cortical/hippocampal neurons or SH-SY5Y cells was biotinylated with sulfo-NHS-SS-biotin (Pierce), according to the manufacturer's instructions. The samples were subsequently subjected to immunocytochemical study or pull-down assay. Biotinylated cell surface proteins were pulled down using Biotin-Capture beads (Adar Biotech).

Immunocytochemical Study—To visualize and quantify neprilysin localization in cortical/hippocampal neurons, the cells were infected with SFV-hNEP, and the cell surface was

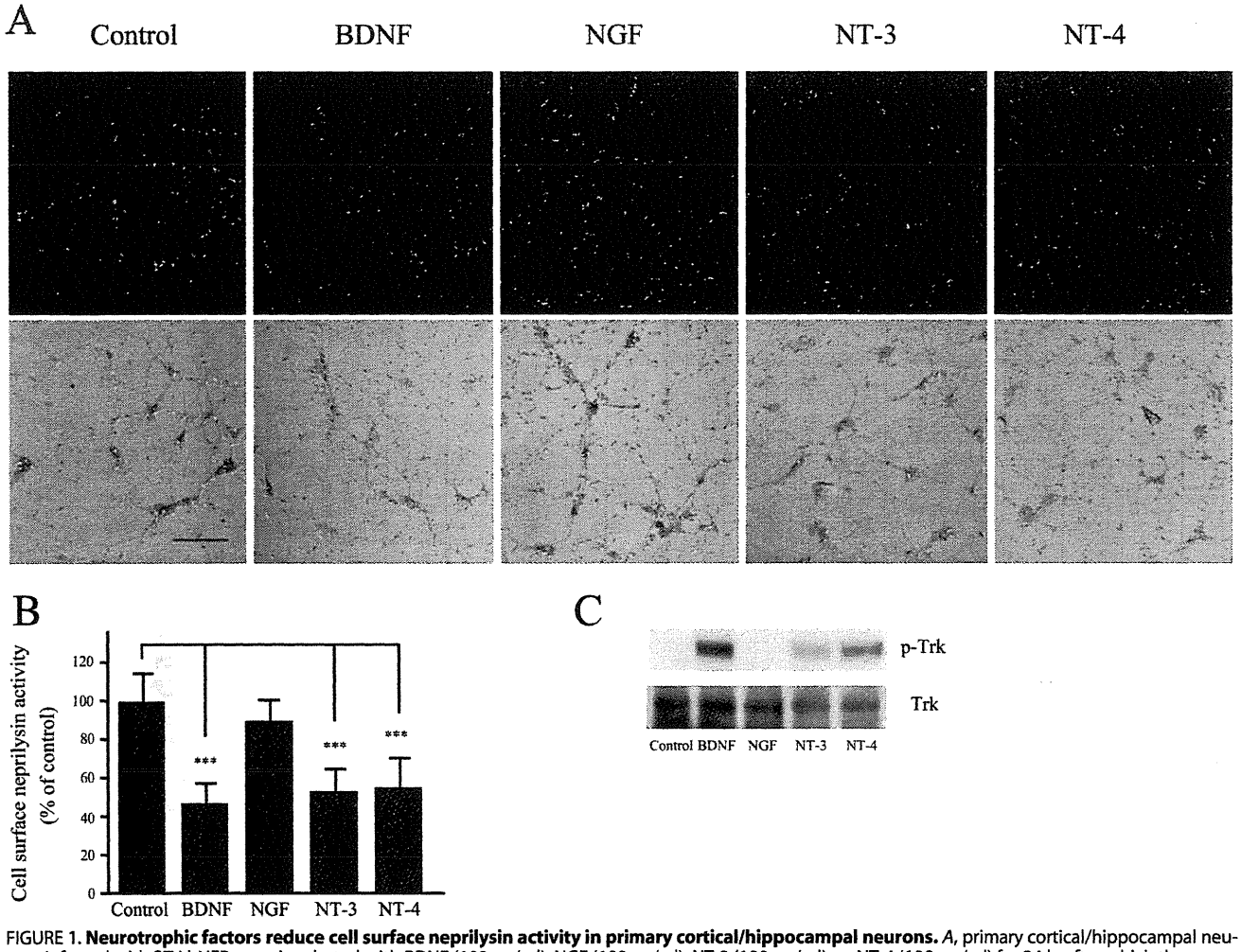

FIGURE 1. **Neurotrophic factors reduce cell surface neprilysin activity in primary cortical/hippocampal neurons.** *A*, primary cortical/hippocampal neurons infected with SFV-hNEP were incubated with BDNF (100 ng/ml), NGF (100 ng/ml), NT-3 (100 ng/ml), or NT-4 (100 ng/ml) for 24 h, after which they were subjected to the neprilysin activity-staining assay. The *top panels* show fluorescence images representing neprilysin activity, and the *bottom panels* show phase-contrast images merged with the *top panels*. *Scale bar*, 100 μm. *B*, quantification of the fluorescence signal areas, indicated as average ± S.D. (*error bars*) ($n = 5$). ***, $p < 0.01$ compared with control. *C*, primary neurons were incubated with BDNF (100 ng/ml), NGF (100 ng/ml), NT-3 (100 ng/ml), or NT-4 (100 ng/ml) for 30 min and then subjected to Western blot analysis to measure the phosphorylation level of the neurotrophic factor receptor, Trk, using antibodies against Trk receptor (*bottom*) and phosphorylated Trk (*p-Trk*; *top*). At least three independent experiments were repeated.

labeled with biotin. The cells grown on coverslips were fixed with 100% ice-cold MeOH for 10 min at −20 °C and permeabilized in 100% ice-cold acetone for 1 min at −20 °C. After blocking with blocking buffer (phosphate-buffered saline containing 5% skim milk, 5% goat serum, and 0.05% Tween 20) for 30 min at room temperature, the samples were incubated with primary anti-human neprilysin antibody (1:100, Novocastra) in blocking buffer for 1 h at room temperature, followed by secondary anti-mouse Alexa 488 (1:500, Invitrogen) and Streptavidin-Alexa 546 (1:500; Molecular Probes) antibody for 30 min at room temperature. The fluorescence signals observed by confocal microscopy were quantified by counting signal dots, as described previously (27).

Immunoprecipitation and Western Blot Analysis—Cell lysates from primary cortical/hippocampal neurons infected with SFV-hNEP were immunoprecipitated with mouse monoclonal anti-human neprilysin (SN5c/L4-1A1, Ancell). Samples were subjected to Western blot analysis using the following antibodies: phospho-human neprilysin antibodies (supplemental Fig. S3), anti-human neprilysin (56C6, Novocastra), anti-mouse neprilysin (421126, Techne), antibodies recognizing the N-terminal region of APP (22C11, Chemicon) or the C-terminal region of APP (A8717, Sigma), anti-PP1A (Thr(P)-320) (EP1512Y, Novus), anti-PP1α (Santa Cruz Biotechnology, Inc., Santa Cruz, CA), anti-phospho-TrkA (Tyr-490, Cell Signaling), anti-Trk (B-3, Cell Signaling), anti-phospho-Erk1/2 (Thr-202/Tyr-204, Cell Signaling), anti-Erk1/2 (Cell Signaling), anti-Myc (9B11, Cell Signaling), anti-G3PDH/GAPDH (Trevigen), or anti-β-actin (AC-15, Sigma-Aldrich).

Aβ ELISA—Conditioned medium from control cortical/hippocampal neurons or those treated with neurotrophic factors for 24 h and from SH-SY5Y cells transiently expressing wild-type neprilysin (WT-NEP), S6A-NEP, WT-PP1a, and T320A-PP1a were collected, and guanidine HCl was added as described previously (4). In order to achieve a measurable level of Aβ40 in the conditioned medium from SH-SY5Y cells transfected with WT-NEP or S6A-NEP, 200 pM Aβ40 peptide was added to the samples. Samples were analyzed using Aβ-ELISA kits (Wako)

to quantify Aβ40 and Aβ42, according to the manufacturer's instructions.

Statistical Analysis—All of the values are presented as mean ± S.D. Statistical analysis was performed by one-way analysis of variance with Scheffe's F test.

RESULTS

Neurotrophic Factors Reduce Neprilysin Activity via MAPK Signal Transduction—Membrane-bound neprilysin located on the cell surface participates in extracellular Aβ degradation and therefore plays a key role in Aβ metabolism. We have previously established an activity-staining method for primary neurons that visualizes neprilysin activity on the cell surface (18, 25). In a search for regulators of neprilysin activity, we identified somatostatin, which was found to exert an up-regulatory effect (18). To further unravel the mechanisms regulating neprilysin activity, we screened the neurotrophic factors BDNF, NGF, NT-3, and NT-4 using our activity-staining technique on primary cortical/hippocampal neurons. Representative images of such activity-staining experiments are shown in Fig. 1. Interestingly, BDNF, NT-3, and NT-4 all significantly reduced neprilysin activity, whereas NGF had no effect. However, given that cortical/hippocampal neurons do not express the TrkA receptor subtype to which NGF binds (28), we also examined the effect of NGF on primary neurons derived from the striatum. Indeed, exposing striatal primary neurons to NGF induced a reduction in neprilysin activity (supplemental Fig. S1, *A* and *B*). To confirm activation of the signal transduction pathway leading to a reduction in neprilysin, phosphorylation of Tyr-490 in Trk was measured (29). Upon exposure of the primary neurons to BDNF, NGF, NT-3, or NT-4, phosphorylation of Trk significantly increased (Fig. 1*C* and supplemental Fig. S1*C*), indicating that the Trk receptors were activated.

To further elucidate the Trk receptor-induced transduction pathway, we next investigated the effects of U0126, LY294002, and calphostin C, inhibitors of MAPK/ERK kinase 1/2 (MEK1/2), phosphatidylinositol-3 kinase, and protein kinase C, respectively, on cell surface neprilysin activity (30). First, we co-treated neurons with BDNF, NGF, NT-3, or NT-4 together with U0126 and found that U0126 completely inhibited the reduction in cell surface neprilysin activity induced by the neurotrophic factors (Fig. 2), indicating the involvement of MAPK/ERK kinase in the signaling pathway. We then focused on NT-3 because it binds to all Trk receptor subtypes (*i.e.* TrkA, -B, and -C) (28). Simultaneous treatment of neurons with NT-3 and calphostin C did not inhibit the reduction in neprilysin activity. Finally, LY294002 treatment alone produced a decrease in cell surface neprilysin activity. However, because LY294002 in combination with NT-3 did not inhibit the NT-3-induced reduction in neprilysin activity (supplemental Fig. S1*D*), it is possible that the effect of LY294002 involves a pathway independent of the Trk signaling pathway. Thus, together these results indicate that neurotrophic factors reduce cell surface neprilysin activity in neurons via the MEK/ERK signaling pathway.

Although binding of neurotrophic factors to Trk receptors is known to activate the MAPK pathway within 30 min (31) (Fig. 1*C*), the levels of cell surface neprilysin activity remained unaltered 30 min after the addition of the neurotrophic factors (supplemental Fig. S1*E*). Rather, the effect became clearly visible 24 h poststimulation (Fig. 1, *A* and *B*). Taken together, these findings indicate that neurotrophic factors reduce cell surface neprilysin activity by binding to neuronal Trk receptors and subsequent activation of the MAPK pathway. The mechanistic explanation behind the delayed effect is currently not known but could include changes in, for example, gene expression of additionally required factors.

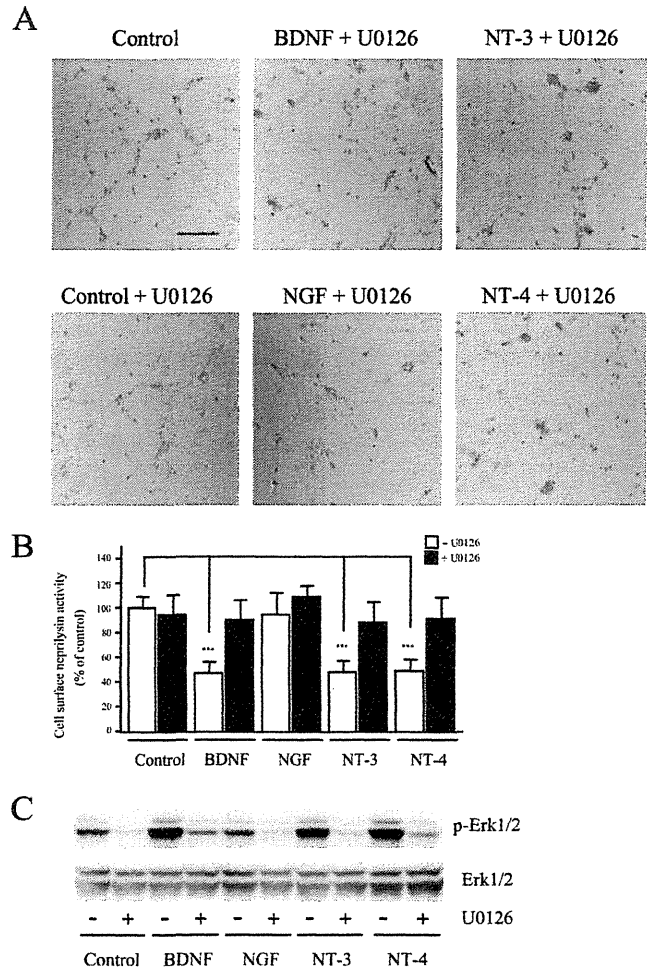

FIGURE 2. **Reduction of neprilysin activity by neurotrophic factors involves the MEK1/2 signaling pathway.** *A*, primary cortical/hippocampal neurons infected with SFV-hNEP were co-incubated with BDNF (100 ng/ml), NGF (100 ng/ml), NT-3 (100 ng/ml), or NT-4 (100 ng/ml) and the MEK1/2 inhibitor U0126 (1 μM), for 24 h, after which they were subjected to the neprilysin activity-staining assay. Representative fluorescence images merged with phase-contrast images are shown. *Scale bar*, 100 μm. *B*, quantification of the fluorescence signal derived from neprilysin activity was performed, and the results are presented as average ± S.D. (*error bars*) ($n = 5$). ***, $p < 0.01$ compared with control. *C*, primary neurons were incubated with or without U0126, as indicated, and neurotrophic factors for 30 min and were then subjected to Western blot analysis to measure the phosphorylation levels of MAPK using antibodies against Erk1/2 (*bottom*) and phosphorylated Erk1/2 (*p-Erk1/2; top*). At least three independent experiments were repeated.

Effect of NT-3 on Aβ Levels—A reduction in neprilysin induced by neurotrophic factors would presumably lead to increased Aβ levels. We therefore measured Aβ levels in conditioned medium from primary neurons infected with SFV-hNEP, using the same conditions as for the activity assay. How-

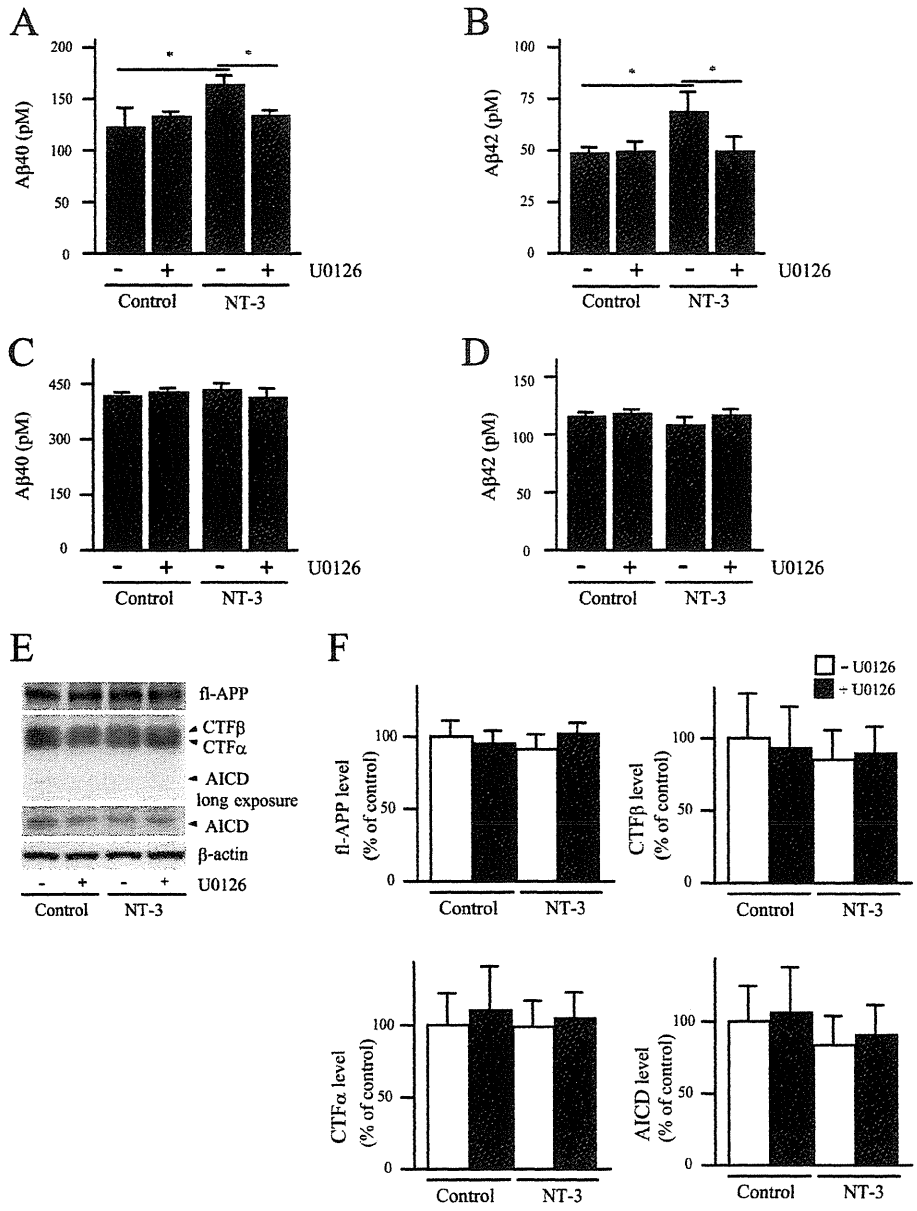

FIGURE 3. **NT-3 induces increased Aβ levels via the MEK/ERK pathway.** *A–D*, the culture medium of primary neurons derived from wild-type (*A* and *B*) or NEP-deficient mouse embryos (*C* and *D*) was collected 24 h after NT-3 (100 ng/ml) treatment with or without U0126 (1 μM) and then subjected to Aβ ELISA. Aβ40 (*A* and *C*) and Aβ42 (*B* and *D*) levels were measured using an Aβ-ELISA kit. Each *column* with *error bar* represents the mean ± S.D. ($n = 4$). *, $p < 0.05$ compared with control and co-treatment. *E* and *F*, the effect of neurotrophic factors on Aβ generation was investigated by measuring the levels of full-length APP (*fl-APP*), CTFα, CTFβ, APP intracellular domain (*AICD*), and β-actin in the primary neurons by Western blot. Intensities of each band were quantified by densitometric analysis, and data represent the mean ± S.D. ($n = 5$).

ever, due to the high viral expression of neprilysin, the Aβ levels were too low to be detected. Therefore, we instead measured the conditioned medium from non-infected primary cortical/hippocampal neurons. NT-3 treatment significantly increased the steady-state levels of Aβ40 and Aβ42, an effect that was abolished by the addition of U0126 (Fig. 3, *A* and *B*). Importantly, treating primary neurons derived from neprilysin-deficient mice with NT-3 did not affect Aβ levels, showing that the increased Aβ levels generated from wild-type neurons are due specifically to a decrease in neprilysin activity (Fig. 3, *C* and *D*). Furthermore, full-length APP levels and the levels of the C-terminal fragments of APP, CTFα, CTFβ, and APP intracellular domain, which are produced by α-, β- and γ-secretase, respectively, and used as an index of secretase activity (32) were not altered by NT-3 treatment (Fig. 3, *E* and *F*). These results together suggest that the increased steady-state levels of Aβ upon NT-3 treatment are due specifically to a decrease in cell surface neprilysin activity rather than increased Aβ generation in the neurons. Finally, to ascertain that the increased Aβ levels observed upon NT-3 treatment were specifically due to decreased levels of cell surface neprilysin, the levels of the Aβ-degrading enzymes endothelin-converting enzyme-1 (33) and insulin-degrading enzyme (34) were investigated. Neither the levels of endothelin-converting enzyme-1 and insulin-

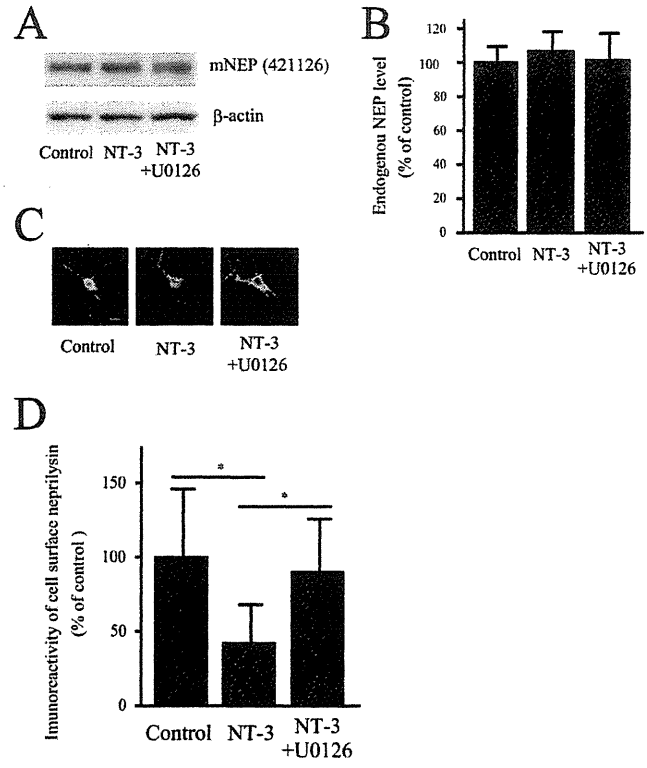

FIGURE 4. **NT-3 regulates neprilysin localization via the MEK/ERK pathway.** *A* and *B*, the effect of NT-3 on expression levels of neprilysin in primary neurons was analyzed by Western blot analysis. The experiments were repeated four times, and the results are presented as mean values ± S.D. (*error bars*). *C* and *D*, double staining for neprilysin and biotinylated proteins located on the cell surface. Primary cortical neurons infected with SFV-hNEP were treated with NT-3 (100 ng/ml) for 24 h. The cell surface proteins were subsequently cross-linked with biotin, after which the cells were double-stained with neprilysin antibody (56C6; *green*) and Alexa 546-conjugated streptavidin (*red*). The images of the *green* and the *red* signals were merged, *yellow* representing cell surface neprilysin. *Scale bar*, 50 μm. The ratio of cell surface neprilysin levels was quantified by image analysis. Data represent the mean ± S.D. ($n = 15$). *, $p < 0.05$ compared with control and co-treatment.

degrading enzyme nor the activity of insulin-degrading enzyme were affected by NT-3 treatment (supplemental Fig. S2, *A* and *B*). These data, together with the lack of changes in Aβ levels secreted from primary neurons prepared from neprilysin knock-out mice and stimulated with neurotrophic factors, lead us to conclude that decreased levels in cell surface neprilysin expression are responsible for the increased Aβ levels.

NT-3 Alters Neprilysin Localization in Neurons—To address whether the NT-3-induced reduction in neprilysin was due to changes in neprilysin expression, we quantified neprilysin levels in whole-cell lysates before and after NT-3 treatment. Western blot data clearly showed that neprilysin expression levels were not altered after NT-3 treatment (Fig. 4, *A* and *B*). Therefore, we next performed immunocytochemical experiments to visualize neprilysin in the neurons. Proteins located on the cell surface were biotinylated, after which the cells were immunocytochemically stained with avidin and anti-neprilysin antibody and analyzed as described under "Experimental Procedures." Quantitative image analysis revealed that the level of neprilysin located on the cell surface was significantly reduced upon NT-3 treatment (Fig. 4, *C* and *D*). Importantly, the addition of U0126 restored this level to normal. Taken together, these results indicate that neurotrophic factors modulate neprilysin localization through MEK/ERK signaling, without affecting neprilysin expression levels, leading to a decrease in cell surface neprilysin activity and ultimately resulting in increased extracellular Aβ levels.

MEK/ERK Signaling Modulates the Phosphorylation State of the Neprilysin Intracellular Domain—The localization of plasma membrane-associated proteins is often regulated by phosphorylation/dephosphorylation at the intracellular domain (ICD) of the protein (35). Because neprilysin is a type II membrane protein, its N-terminal side is located in the cytoplasmic lumen. As shown in Fig. 5*A*, there are five potential amino acid residues in human neprilysin and four in mouse neprilysin ICD (NEP-ICD) that could possibly be phosphorylated. In order to accurately determine the phosphorylation state of the NEP-ICD, we first generated the phosphoserine- and phosphothreonine-specific antibodies pS4-NEP, pS6-NEP, pT11-NEP, pT15-NEP, and pT25-NEP, which specifically recognize individual phosphorylated threonine and serine residues in the NEP-ICD, respectively. The specificities of these antibodies are summarized in supplemental Fig. S3. We then probed cell extracts of primary neurons using this battery of phospho-antibodies. Although the endogenous expression level of neprilysin is low, we were able to detect phosphorylation of Ser-4, Ser-6, and Thr-11 in neprilysin (Fig. 5). We were not able to detect pT25-NEP due to limited affinity of the antibody. Interestingly, upon exposing primary neurons to NT-3, phosphorylation of Ser-6 increases significantly. Simultaneously treating the cells with NT-3 and U0126 inhibited the increase in phosphorylation of Ser-6 induced by NT-3, implying that the MAPK pathway is involved in the regulation of NEP-ICD phosphorylation (Fig. 5, *B* and *C*).

Because the endogenous neprilysin level in primary neurons is low and our aim was to study the regulatory mechanism of human neprilysin, we continued our studies using SFV-hNEP-infected primary neurons. After infection, we investigated the phosphorylation state of NEP-ICD. Consistent with phosphorylation of Ser-6 of endogenous neprilysin, we detected that overexpressed human neprilysin also was phosphorylated at Ser-6 upon treatment with NT-3. Further, the effect was inhibited by the addition of U0126. In addition, a trend toward increased Ser-4 phosphorylation was detected together with increased phosphorylation of Thr-15 (Fig. 5, *B* and *C*). Subsequently, we examined whether neprilysin localized to the cell surface exhibits different phosphorylation statuses compared with intracellularly located neprilysin. Biotinylated proteins located on the cell surface of SFV-hNEP-infected primary neurons were first pulled down from cell lysates using Biotin-Capture beads, after which intracellular neprilysin was collected using a neprilysin-specific antibody. Although all potential phosphorylation sites in the NEP-ICD of intracellularly located neprilysin were phosphorylated, no phosphorylation of Ser-6 or Thr-25 could be detected in neprilysin present in the cell surface fraction (Fig. 5*D*). These results together indicated that treating the cells with NT-3 for 24 h resulted in extensive phosphorylation of Ser-6 and Thr-15 of cell surface-located neprilysin. Although activation of Trk receptors was detected 30 min

after the addition of NT-3 to the cells, there was no difference in the phosphorylation state of NEP-ICD after a 30-min treatment by NT-3 (data not shown). The reasons behind the delayed effect are currently not known. Furthermore, the increase in phosphorylation of Ser-4, Ser-6, and Thr-15 induced by NT-3 was inhibited by the addition of U0126, indicating the involvement of MAPK in the signaling pathway (Fig. 5, *B* and *C*). Together, the data indicate that phosphorylation of Ser-6 is involved in the regulation of cell surface neprilysin.

To further clarify the role of human NEP-ICD phosphorylation in neprilysin activity, we generated five mutants in which

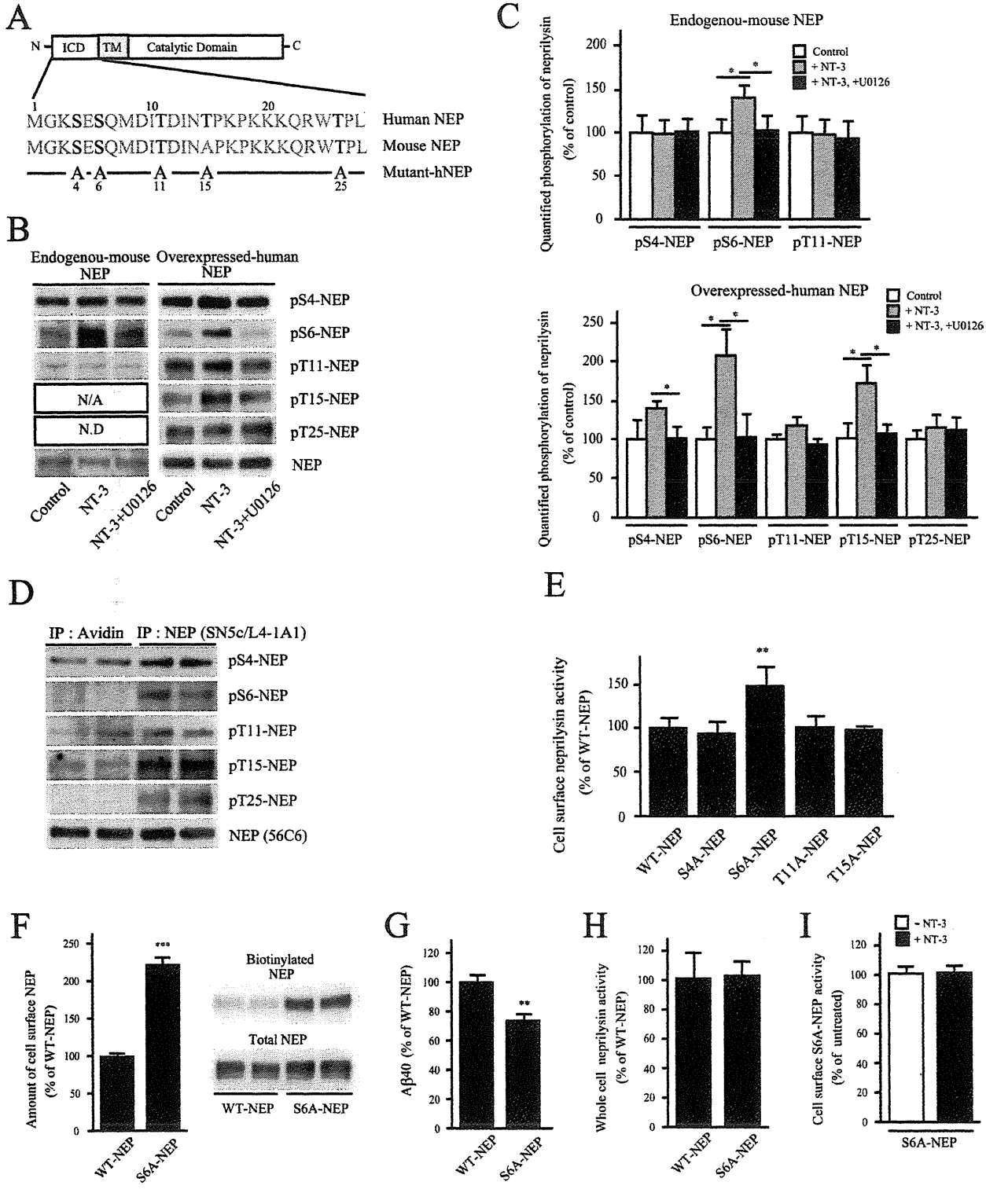

the putative serines/threonines in the NEP-ICD were substituted with alanines (*i.e.* S4A-, S6A-, T11A-, T15A-, and T25A-NEP, respectively) (Fig. 5*A*). The selection of a cell line for the mutational analysis was based on two criteria: 1) it should be a human neuronal cell line, and 2) it should express endogenous neprilysin to assure that the regulatory mechanisms of neprilysin are preserved. The endogenous expression of neprilysin in SH-SY5Y was confirmed with Western blot (Fig. S5*A*). Thus, the mutants were introduced into SH-SY5Y cells, and cell surface neprilysin activity was measured and normalized to expression levels. Interestingly, S6A-NEP transfectants showed significantly higher cell surface activity than S4A-, T11A-, T15A-, and WT-NEP transfectants (Fig. 5*E* and supplemental Fig. S4). The effect of T25A-NEP on neprilysin activity could not be evaluated due to its low expression (supplemental Fig. S5). We also subsequently measured the amount of cell surface-located S6A-NEP and found it to be significantly higher than that of WT-NEP (Fig. 5*F*). In accordance with the increased cell surface activity of S6A-NEP, the extracellular Aβ40 level in conditioned medium from S6A-NEP transfectants was significantly lower than that for WT-NEP transfectants (Fig. 5*G*). Furthermore, the total neprilysin activity, normalized to expression levels, in whole-cell lysates from WT-NEP and S6A-NEP transfectants were similar (Fig. 5*H*). This indicates that the increase in cell surface neprilysin activity observed in the case of S6A-NEP was not due to an allosteric effect induced by the mutation. Last, the cell surface neprilysin activity of S6A-NEP transfectants was not affected by NT-3 treatment (Fig. 5*I*). Taking all of the data together, we conclude that phosphorylation of Ser-6 of the NEP-ICD regulates neprilysin localization and thereby neprilysin cell surface activity via MEK/ERK signaling.

PP1a Facilitates Cell Surface Neprilysin Activity—Given that phosphorylation of Ser-6 in the NEP-ICD influences neprilysin cell surface localization, we next evaluated the effects of different phosphatase activities on neprilysin localization and activity. Primary cortical/hippocampal neurons infected with SFV-hNEP were treated with the following specific inhibitors for serine/threonine phosphatases: tautomycetin (PP1a inhibitor), fostriecin and okadaic acid (PP2A inhibitors), and cyclosporin A and FK-506 (PP2B/calcineurin inhibitors). Interestingly, treatment with the PP1a inhibitor tautomycetin resulted in significantly increased phosphorylation of the S6-NEP-ICD (Fig. 6, *A* and *B*) and decreased cell surface neprilysin activity (Fig. 6*C*). In addition to S6-NEP-ICD, phosphorylation of S4- and T11-NEP-ICDs was also increased by tautomycetin. However, phosphorylation of Ser-4 and Thr-11 did not influence cell surface neprilysin activity (Fig. 5 and supplemental Fig. S6).

The increased phosphorylation of Ser-6 upon PP1a inhibition suggests an association of neprilysin and PP1a. Previously, PTEN (phosphatase and tensin homolog deleted from chromosome 10), which is a tumor suppressor and acts as a tyrosine phosphatase, has been shown to be associated with the NEP-ICD (36). Interestingly, an amino acid sequence found in the NEP-ICD, KKKQRW, is similar to a PP1a-interacting sequence (37, 38). This finding prompted us to investigate a possible interaction between neprilysin and PP1a. We therefore performed immunoprecipitation experiments using SH-SY5Y cell lysates from mock and WT-NEP transfectants. The results revealed that neprilysin co-immunoprecipitates not only with PTEN but also with PP1a, indicating that the proteins are directly or indirectly associated (Fig. 6*D*).

To confirm the role of PP1a in neprilysin dephosphorylation and localization, and because PP1a is activated by dephosphorylation at the threonine 320 residue, we prepared a constitutive active mutant PP1a, which harbors a T320A mutation (Fig. 6*E*) (24). Expression of both WT-PP1a and T320A-PP1a in SFV-hNEP-infected SH-SY5Y cells induced an increase in cell surface neprilysin activity compared with mock transfectants. Moreover, constitutive active T320A-PP1a transfectants exhibited significantly higher cell surface neprilysin activity compared with WT-PP1a transfectants (Fig. 6*F*).

In addition, extracellular Aβ levels were significantly reduced by both WT-PP1a and T320A-PP1a expression (Fig. 6*G*). Taken together, these results suggest that activation of PP1a increases cell surface neprilysin activity/localization is due, at least partly, to dephosphorylation of Ser-6 in the NEP-ICD.

DISCUSSION

Pharmacological maintenance or enhancement of the major Aβ-degrading enzyme neprilysin during aging could offer a possible treatment for the prevention of AD. Accumulating evi-

FIGURE 5. **Dephosphorylation of the neprilysin intracellular domain localizes neprilysin to the cell surface.** *A*, scheme of human and mouse neprilysin domain structure and the N-terminal amino acid sequences corresponding to the neprilysin intracellular domain. *ICD* and *TM*, intracellular domain and transmembrane domain of neprilysin, respectively. Potential phosphorylation sites are indicated in *boldface type*. *Below*, the substituted serines/threonines to alanines are indicated in the five phosphoneprilysin mutants, S4A-, S6A-, T11A-, T15A-, and T25A-NEP. *B*, effects of NT-3 on the phosphorylation state of the intracellular domain of neprilysin. Primary neurons (*left*) were untreated or treated with NT-3 (100 ng/ml) or NT-3 together with U0126 for 24 h, as indicated, after which neprilysin was immunoprecipitated from 1 mg of cell lysate with neprilysin antibody, and the immunoprecipitates were analyzed by immunoblotting with phosphoneprilysin antibodies. Primary neurons expressing human neprilysin by infection with SFV-hNEP (*right*) were treated the same way as the non-infected primary neurons, as indicated. 150 μg of cell lysate was immunoprecipitated and immunoblotted with phosphoneprilysin antibodies, as indicated to the *right*. *N/A*, not applicable; *N.D*, not determined. *C*, densitometric quantification of Western blot data in *B*. Data represent the mean ± S.D. (*error bars*) ($n = 3$). *, $p < 0.05$, treated sample compared with non-treated or co-treated. *D*, cell surface-located proteins were biotinylated and pulled down using streptavidin beads, followed by immunoprecipitation (*IP*) of non-biotinylated neprilysin using a neprilysin antibody. Immunoprecipitates were subjected to Western blot analysis using the phosphoneprilysin antibodies pS4-NEP, pS6-NEP, pT11-NEP, pT15-NEP, pT25-NEP, and NEP (56C6). Western blot data of samples from two independent experiments are shown. At least three independent experiments were performed, and a similar band pattern was repeatedly verified. *E*, cell surface neprilysin activity of SH-SY5Y cells transiently expressing WT-, S4A-, S6A-, T11A-, T15A-, or T25A-NEP were evaluated using suc-Ala-Ala-Phe-MCA substrate. The neprilysin activities were normalized to neprilysin expression levels quantified by Western blot. Data represent the mean ± S.D. ($n = 3$). **, $p < 0.01$ compared with WT-NEP. *F*, SH-SY5Y cells transiently expressing WT-NEP or S6A-NEP were biotinylated, and the amount of biotinylated neprilysin was evaluated by a pull-down assay. Data represent the mean ± S.D. ($n = 3$). ***, $p < 0.01$ compared with WT-NEP. *G*, Aβ levels in the conditioned medium from SH-SY5Y cells transiently expressing WT-NEP or S6A-NEP. Data represent the mean ± S.D. ($n = 4$). **, $p < 0.01$ compared with WT-NEP. *H*, neprilysin activity in whole-cell lysates from WT-NEP and S6A-NEP transfectants was measured. Data represent the mean ± S.D. ($n = 3$). *I*, the effect of NT-3 on cell surface S6A-NEP activity. SH-SY5Y cells transiently expressing S6A-NEP were treated with NT-3 for 24 h. Cell surface neprilysin activity was measured using suc-Ala-Ala-Phe-MCA substrate. Data represent the mean ± S.D. ($n = 3$).

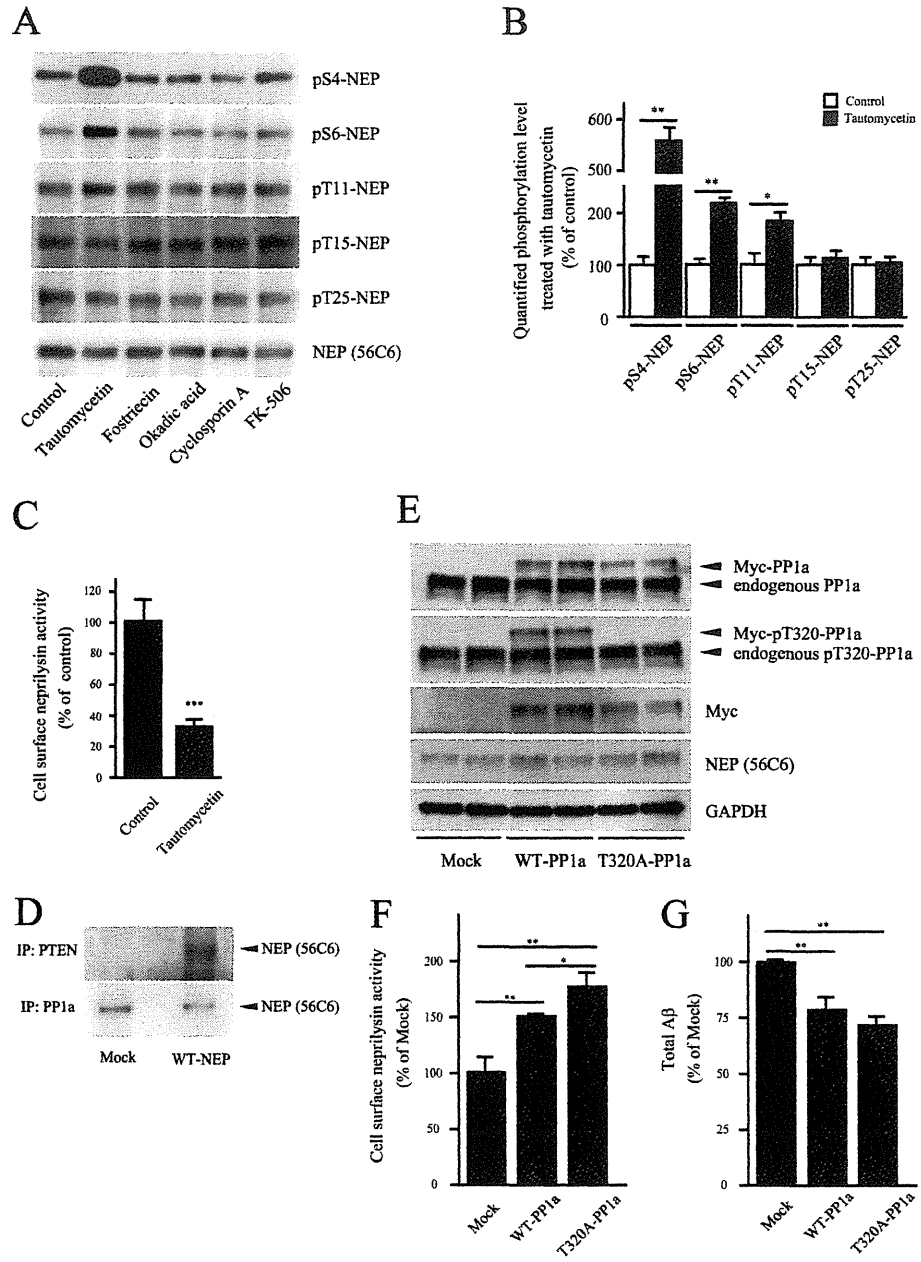

FIGURE 6. **PP1a regulates neprilysin activity through dephosphorylation.** *A*, primary neurons infected with SFV-hNEP were treated with specific inhibitors of serine/threonine phosphatases, tautomycetin (1 μM), fostriecin (100 nM), okadaic acid (10 nM), cyclosporin A (1 μM), and FK-506 (1 μM), and the phosphorylation state of neprilysin was measured by immunoprecipitation using a neprilysin antibody and immunoblot with phosphospecific antibodies. *B*, densitometric quantification of phosphorylation levels after tautomycetin treatment for 24 h as analyzed by Western blot in *A*. Data represent the mean ± S.D. (*error bars*) ($n = 3$). *, $p < 0.05$; **, $p < 0.01$ compared with non-treated. *C*, the effect of tautomycetin on cell surface neprilysin activity in primary neurons infected with SFV-hNEP. Data represent the mean ± S.D. ($n = 3$). **, $p < 0.01$ compared with control. *D*, immunoprecipitation (*IP*) of SH-SY5Y cell lysates with PTEN and PP1a antibodies. SH-SY5Y cells were transfected with a mock or WT-NEP expression vector. Lysates were prepared and immunoprecipitated using PTEN and PP1a antibodies as indicated. The immunoprecipitates were subjected to Western blot analysis, using anti-neprilysin antibody for detection. *E*, verification of WT- and T320A-PP1a expression in SH-SY5Y transfectants by Western blot and using antibodies as indicated to the *right*. *F*, the effect of PP1a activation on cell surface neprilysin activity. SH-SY5Y cells infected with SFV-hNEP were transfected with WT- or T320A-PP1a followed by measurement of cell surface neprilysin activity. Data represent the mean ± S.D. ($n = 4$). *, $p < 0.05$; **, $p < 0.01$ compared with control. *G*, effect of PP1a activation on Aβ levels. The Aβ levels in conditioned medium from WT- and T320A-PP1a-transfected SH-SY5Y cells, infected with SFV-hNEP, were quantified by ELISA. Data represent the mean ± S.D. ($n = 4$). **, $p < 0.01$ compared with control.

dence indicates the feasibility of a neprilysin-based approach. For example, overexpression of neprilysin leads to a decrease in Aβ load and improved memory in AD model mice. Another factor that argues in favor of a neprilysin-based treatment is the limited number of possible side effects. For example, the levels of neuropeptides in neprilysin knock-out mice are unaltered, indicating that proteases other than neprilysin are involved in their metabolism. Furthermore, neprilysin transgenic mice do not display other behavioral abnormalities (15–17, 39). However, in order to develop a neprilysin-based AD treatment, it is

essential to have a more detailed understanding of the mechanism of neprilysin activation and to identify a regulator of neprilysin activity.

In this report, we show that neurotrophic factors reduce cell surface neprilysin activity (Fig. 1 and supplemental Fig. S1) through regulation of cell surface neprilysin localization (Fig. 4) and that the reduction of neprilysin activity leads to increased Aβ levels (Fig. 3). On the other hand, previous extensive studies have shown that neurotrophic factors, particularly BDNF, exhibit neuroprotective properties that contribute to neuronal survival and memory formation in both rodent and primate models of AD through amyloid-independent mechanisms (40). In addition, BDNF also supports neural stem cells, which have been demonstrated to improve cognition in a transgenic model of AD (41). Furthermore, oligomeric Aβ has been shown to decrease cortical BDNF levels and synaptic function in an AD model mouse (42, 43). These findings together indicate that BDNF would be a useful adjunct in AD therapy to compensate for decreased levels of this neurotrophic factor in the brain and to ameliorate symptoms in the late stages of disease, whereas a strategy involving neprilysin activation could be effective in preventing or delaying the onset of AD because the facilitation of Aβ clearance would attenuate synaptic dysfunction and the reduction in BDNF levels. In fact, with accumulating knowledge, it appears that any treatment for AD is likely to be directed at several targets simultaneously. Our data show that a strategy involving any neurotrophic factor would have as a side effect increased Aβ levels that would have to be taken into account.

The use of neurotrophic factors in this study enabled us to unravel some of the mechanisms controlling neprilysin activity. We found that cell surface neprilysin activity is regulated through the localization of neprilysin to the cell surface, a process that in turn is mediated by phosphorylation/dephosphorylation of the NEP-ICD (Figs. 4 and 5). The regulation of neprilysin activity also involved MEK/ERK signaling, which resulted in phosphorylation of Ser-6 in the NEP-ICD (Figs. 2 and 5), although it remains unclear whether ERK directly phosphorylates the NEP-ICD. Interestingly, casein kinase 2 has been reported to act as a kinase for S6-NEP-ICD phosphorylation (44). Moreover, increased phosphorylation of neprilysin appeared after 24 h of stimulation, indicating that the expression of additional unknown factors might be required.

Although the mechanism remains unclear, metabolism of neprilysin itself would also influence its cell surface activity. Interestingly, T25A-NEP mutant protein could not be detected in transfected cells, despite the presence of the mRNA (supplemental Fig. S5). Speculatively, dephosphorylation of Thr-25 might induce degradation of neprilysin in the cells, as part of a quality control mechanism in the metabolic pathway of neprilysin, although Thr-25 was found to be dephosphorylated in neprilysin located at the cell surface (Fig. 5*D*). Alternatively, the introduced mutation could destabilize the protein and induce aggregation, although the S6A/T25A double mutant was normally expressed in the transfectants (data not shown).

The addition of the PP1a inhibitor tautomycetin to primary cortical/hippocampal neurons extensively increased the phosphorylation state of the NEP-ICD (Fig. 6, *A* and *B*) and reduced cell surface neprilysin activity (Fig. 6*C*). A closer examination of the NEP-ICD amino acid sequence revealed a peptide sequence, KKKQRW, similar to the PP1a binding motif, suggesting that the NEP-ICD might be a target of PP1a. Indeed, PP1a was found to be associated with neprilysin in SH-SY5Y cell extracts, and overexpression of PP1a stimulated cell surface neprilysin activity, leading to reduced Aβ levels (Fig. 6, *D–G*). Therefore, activation of PP1a (*e.g.* pharmacologically) would be a possible strategy to increase cell surface neprilysin activity. Interestingly, it has been reported that PP1a activity was regulated by DARPP32, an endogenous regulator of PP1a (45), and that DARPP32 levels are reduced in the brains of somatostatin receptor-1 (SSTR1) and SSTR5 double knock-out mice (46). These observations, considered together with our previous data showing that presynaptic localization of neprilysin is significantly decreased in the hippocampus of somatostatin-deficient mice (18), indicate that somatostatin possibly regulates neprilysin activity through PP1 activity. Thus, SSTR agonists might be successful drug candidates for the treatment of AD.

With the development of new gene therapy technologies, application of a neprilysin gene transfer strategy could be a potential way to decrease Aβ levels and delay the onset of amyloidosis. Considering the increased activity of S6-NEP, an alternative would be to introduce the S6A-NEP mutant, possibly leading to even more efficient Aβ degradation compared with that of WT-NEP.

In conclusion, our results show that the phosphorylation state of the intracellular domain regulates cell surface neprilysin activity and extracellular Aβ levels due to the modulation of neprilysin localization. We propose that enhancing cell surface neprilysin activity, for example by maintaining S6 of the NEP-ICD in a dephosphorylated state, either through activation of phosphatases or through inhibition of the kinase responsible for phosphorylation at the S6-NEP-ICD, would be beneficial for the prevention of Aβ amyloidosis.

Acknowledgment—We thank Dr. C. Gerard for providing neprilysin-deficient mice.

REFERENCES

1. Hardy, J., and Selkoe, D. J. (2002) The amyloid hypothesis of Alzheimer's disease. Progress and problems on the road to therapeutics. *Science* **297,** 353–356
2. Selkoe, D. J. (1994) Alzheimer's disease. A central role for amyloid. *J. Neuropathol. Exp. Neurol.* **53,** 438–447
3. Selkoe, D. J. (1994) Cell biology of the amyloid β-protein precursor and the mechanism of Alzheimer's disease. *Annu. Rev. Cell Biol.* **10,** 373–403
4. Saito, T., Suemoto, T., Brouwers, N., Sleegers, K., Funamoto, S., Mihira, N., Matsuba, Y., Yamada, K., Nilsson, P., Takano, J., Nishimura, M., Iwata, N., Van Broeckhoven, C., Ihara, Y., and Saido, T. C. (2011) Potent amyloidogenicity and pathogenicity of Aβ43. *Nat. Neurosci.* **14,** 1023–1032
5. Saido, T. C. (1998) Alzheimer's disease as proteolytic disorders. Anabolism and catabolism of β-amyloid. *Neurobiol. Aging* **19,** S69–S75
6. Iwata, N., Tsubuki, S., Takaki, Y., Shirotani, K., Lu, B., Gerard, N. P., Gerard, C., Hama, E., Lee, H. J., and Saido, T. C. (2001) Metabolic regulation of brain Aβ by neprilysin. *Science* **292,** 1550–1552
7. Iwata, N., Tsubuki, S., Takaki, Y., Watanabe, K., Sekiguchi, M., Hosoki, E., Kawashima-Morishima, M., Lee, H. J., Hama, E., Sekine-Aizawa, Y., and Saido, T. C. (2000) Identification of the major Aβ1–42-degrading catabolic pathway in brain parenchyma. suppression leads to biochemical and pathological deposition. *Nat. Med.* **6,** 143–150

8. Caccamo, A., Oddo, S., Sugarman, M. C., Akbari, Y., and LaFerla, F. M. (2005) Age- and region-dependent alterations in Aβ-degrading enzymes. implications for Aβ-induced disorders. *Neurobiol. Aging* **26,** 645–654
9. Reilly, C. E. (2001) Neprilysin content is reduced in Alzheimer brain areas. *J. Neurol.* **248,** 159–160
10. Carter, T. L., Pedrini, S., Ghiso, J., Ehrlich, M. E., and Gandy, S. (2006) Brain neprilysin activity and susceptibility to transgene-induced Alzheimer amyloidosis. *Neurosci. Lett.* **392,** 235–239
11. Iwata, N., Takaki, Y., Fukami, S., Tsubuki, S., and Saido, T. C. (2002) Region-specific reduction of Aβ-degrading endopeptidase, neprilysin, in mouse hippocampus upon aging. *J. Neurosci. Res.* **70,** 493–500
12. Yasojima, K., Akiyama, H., McGeer, E. G., and McGeer, P. L. (2001) Reduced neprilysin in high plaque areas of Alzheimer brain. A possible relationship to deficient degradation of β-amyloid peptide. *Neurosci. Lett.* **297,** 97–100
13. Huang, S. M., Mouri, A., Kokubo, H., Nakajima, R., Suemoto, T., Higuchi, M., Staufenbiel, M., Noda, Y., Yamaguchi, H., Nabeshima, T., Saido, T. C., and Iwata, N. (2006) Neprilysin-sensitive synapse-associated amyloid-β peptide oligomers impair neuronal plasticity and cognitive function. *J. Biol. Chem.* **281,** 17941–17951
14. Farris, W., Schütz, S. G., Cirrito, J. R., Shankar, G. M., Sun, X., George, A., Leissring, M. A., Walsh, D. M., Qiu, W. Q., Holtzman, D. M., and Selkoe, D. J. (2007) Loss of neprilysin function promotes amyloid plaque formation and causes cerebral amyloid angiopathy. *Am. J. Pathol.* **171,** 241–251
15. Iwata, N., Mizukami, H., Shirotani, K., Takaki, Y., Muramatsu, S., Lu, B., Gerard, N. P., Gerard, C., Ozawa, K., and Saido, T. C. (2004) Presynaptic localization of neprilysin contributes to efficient clearance of amyloid-β peptide in mouse brain. *J. Neurosci.* **24,** 991–998
16. El-Amouri, S. S., Zhu, H., Yu, J., Marr, R., Verma, I. M., and Kindy, M. S. (2008) Neprilysin. An enzyme candidate to slow the progression of Alzheimer's disease. *Am. J. Pathol.* **172,** 1342–1354
17. Leissring, M. A., Farris, W., Chang, A. Y., Walsh, D. M., Wu, X., Sun, X., Frosch, M. P., and Selkoe, D. J. (2003) Enhanced proteolysis of β-amyloid in APP transgenic mice prevents plaque formation, secondary pathology, and premature death. *Neuron* **40,** 1087–1093
18. Saito, T., Iwata, N., Tsubuki, S., Takaki, Y., Takano, J., Huang, S. M., Suemoto, T., Higuchi, M., and Saido, T. C. (2005) Somatostatin regulates brain amyloid β peptide Aβ42 through modulation of proteolytic degradation. *Nat. Med.* **11,** 434–439
19. Saido, T. C., Nagao, S., Shiramine, M., Tsukaguchi, M., Sorimachi, H., Murofushi, H., Tsuchiya, T., Ito, H., and Suzuki, K. (1992) Autolytic transition of μ-calpain upon activation as resolved by antibodies distinguishing between the pre- and post-autolysis forms. *J. Biochem.* **111,** 81–86
20. Saido, T. C., Iwatsubo, T., Mann, D. M., Shimada, H., Ihara, Y., and Kawashima, S. (1995) Dominant and differential deposition of distinct beta-amyloid peptide species, Aβ N3(pE), in senile plaques. *Neuron* **14,** 457–466
21. Pagans, S., Sakane, N., Schnölzer, M., and Ott, M. (2011) Characterization of HIV Tat modifications using novel methyl-lysine-specific antibodies. *Methods* **53,** 91–96
22. Hussain, I., Hawkins, J., Harrison, D., Hille, C., Wayne, G., Cutler, L., Buck, T., Walter, D., Demont, E., Howes, C., Naylor, A., Jeffrey, P., Gonzalez, M. I., Dingwall, C., Michel, A., Redshaw, S., and Davis, J. B. (2007) Oral administration of a potent and selective non-peptidic BACE-1 inhibitor decreases β-cleavage of amyloid precursor protein and amyloid-β production *in vivo*. *J. Neurochem.* **100,** 802–809
23. Shirotani, K., Tsubuki, S., Iwata, N., Takaki, Y., Harigaya, W., Maruyama, K., Kiryu-Seo, S., Kiyama, H., Iwata, H., Tomita, T., Iwatsubo, T., and Saido, T. C. (2001) Neprilysin degrades both amyloid β peptides 1–40 and 1–42 most rapidly and efficiently among thiorphan- and phosphoramidon-sensitive endopeptidases. *J. Biol. Chem.* **276,** 21895–21901
24. Berndt, N., Dohadwala, M., and Liu, C. W. (1997) Constitutively active protein phosphatase 1α causes Rb-dependent G_1 arrest in human cancer cells. *Curr. Biol.* **7,** 375–386
25. Hama, E., Shirotani, K., Iwata, N., and Saido, T. C. (2004) Effects of neprilysin chimeric proteins targeted to subcellular compartments on amyloid β peptide clearance in primary neurons. *J. Biol. Chem.* **279,** 30259–30264
26. Takaki, Y., Iwata, N., Tsubuki, S., Taniguchi, S., Toyoshima, S., Lu, B., Gerard, N. P., Gerard, C., Lee, H. J., Shirotani, K., and Saido, T. C. (2000) Biochemical identification of the neutral endopeptidase family member responsible for the catabolism of amyloid β peptide in the brain. *J. Biochem.* **128,** 897–902
27. Rappoport, J. Z., and Simon, S. M. (2003) Real-time analysis of clathrin-mediated endocytosis during cell migration. *J. Cell Sci.* **116,** 847–855
28. Barbacid, M. (1994) The Trk family of neurotrophin receptors. *J. Neurobiol.* **25,** 1386–1403
29. Segal, R. A., and Greenberg, M. E. (1996) Intracellular signaling pathways activated by neurotrophic factors. *Annu. Rev. Neurosci.* **19,** 463–489
30. Segal, R. A. (2003) Selectivity in neurotrophin signaling. Theme and variations. *Annu. Rev. Neurosci.* **26,** 299–330
31. Loeb, D. M., Tsao, H., Cobb, M. H., and Greene, L. A. (1992) NGF and other growth factors induce an association between ERK1 and the NGF receptor, gp140prototrk. *Neuron* **9,** 1053–1065
32. Zheng, H., and Koo, E. H. (2006) The amyloid precursor protein. Beyond amyloid. *Mol. Neurodegener.* **1,** 5
33. Eckman, E. A., Watson, M., Marlow, L., Sambamurti, K., and Eckman, C. B. (2003) Alzheimer's disease β-amyloid peptide is increased in mice deficient in endothelin-converting enzyme. *J. Biol. Chem.* **278,** 2081–2084
34. Farris, W., Mansourian, S., Chang, Y., Lindsley, L., Eckman, E. A., Frosch, M. P., Eckman, C. B., Tanzi, R. E., Selkoe, D. J., and Guenette, S. (2003) Insulin-degrading enzyme regulates the levels of insulin, amyloid β-protein, and the β-amyloid precursor protein intracellular domain *in vivo*. *Proc. Natl. Acad. Sci. U.S.A.* **100,** 4162–4167
35. Pawson, T., and Scott, J. D. (1997) Signaling through scaffold, anchoring, and adaptor proteins. *Science* **278,** 2075–2080
36. Sumitomo, M., Iwase, A., Zheng, R., Navarro, D., Kaminetzky, D., Shen, R., Georgescu, M. M., and Nanus, D. M. (2004) Synergy in tumor suppression by direct interaction of neutral endopeptidase with PTEN. *Cancer Cell* **5,** 67–78
37. Roy, J., and Cyert, M. S. (2009) Cracking the phosphatase code. Docking interactions determine substrate specificity. *Sci. Signal.* **2,** re9
38. Hurley, T. D., Yang, J., Zhang, L., Goodwin, K. D., Zou, Q., Cortese, M., Dunker, A. K., and DePaoli-Roach, A. A. (2007) Structural basis for regulation of protein phosphatase 1 by inhibitor-2. *J. Biol. Chem.* **282,** 28874–28883
39. Iwata, N., Higuchi, M., and Saido, T. C. (2005) Metabolism of amyloid-beta peptide and Alzheimer's disease. *Pharmacol. Ther.* **108,** 129–148
40. Nagahara, A. H., Merrill, D. A., Coppola, G., Tsukada, S., Schroeder, B. E., Shaked, G. M., Wang, L., Blesch, A., Kim, A., Conner, J. M., Rockenstein, E., Chao, M. V., Koo, E. H., Geschwind, D., Masliah, E., Chiba, A. A., and Tuszynski, M. H. (2009) Neuroprotective effects of brain-derived neurotrophic factor in rodent and primate models of Alzheimer's disease. *Nat. Med.* **15,** 331–337
41. Blurton-Jones, M., Kitazawa, M., Martinez-Coria, H., Castello, N. A., Müller, F. J., Loring, J. F., Yamasaki, T. R., Poon, W. W., Green, K. N., and LaFerla, F. M. (2009) Neural stem cells improve cognition via BDNF in a transgenic model of Alzheimer disease. *Proc. Natl. Acad. Sci. U.S.A.* **106,** 13594–13599
42. Peng, S., Garzon, D. J., Marchese, M., Klein, W., Ginsberg, S. D., Francis, B. M., Mount, H. T., Mufson, E. J., Salehi, A., and Fahnestock, M. (2009) Decreased brain-derived neurotrophic factor depends on amyloid aggregation state in transgenic mouse models of Alzheimer's disease. *J. Neurosci.* **29,** 9321–9329
43. Zheng, Z., Sabirzhanov, B., and Keifer, J. (2010) Oligomeric amyloid-β inhibits the proteolytic conversion of brain-derived neurotrophic factor (BDNF), AMPA receptor trafficking, and classical conditioning. *J. Biol. Chem.* **285,** 34708–34717
44. Siepmann, M., Kumar, S., Mayer, G., and Walter, J. (2010) Casein kinase 2 dependent phosphorylation of neprilysin regulates receptor tyrosine kinase signaling to Akt. *PLoS One* **5,** e13134
45. Greengard, P., Allen, P. B., and Nairn, A. C. (1999) Beyond the dopamine receptor. The DARPP-32/protein phosphatase-1 cascade. *Neuron* **23,** 435–447
46. Rajput, P. S., Kharmate, G., Norman, M., Liu, S. H., Sastry, B. R., Brunicardi, C. F., and Kumar, U. (2011) Somatostatin receptor 1 and 5 double knockout mice mimic neurochemical changes of Huntington's disease transgenic mice. *PLoS One* **6,** e24467

BIOCHEMISTRY
including biophysical chemistry & molecular biology

Article

pubs.acs.org/biochemistry

Human Prefoldin Inhibits Amyloid-β (Aβ) Fibrillation and Contributes to Formation of Nontoxic Aβ Aggregates

Karin Margareta Sörgjerd,[†] Tamotsu Zako,*[,†] Masafumi Sakono,[†] Peter C. Stirling,[‡,∥] Michel R. Leroux,[‡] Takashi Saito,[§] Per Nilsson,[§] Misaki Sekimoto,[§] Takaomi C. Saido,[§] and Mizuo Maeda*[,†]

[†]Bioengineering Laboratory, RIKEN, 2-1 Hirosawa, Wako, Saitama 351-0198, Japan

[‡]Department of Molecular Biology and Biochemistry, Simon Fraser University, 8888 University Drive, Burnaby, BC V5A 1S6, Canada

[§]Laboratory for Proteolytic Neuroscience, RIKEN Brain Science Institute, 2-1 Hirosawa, Wako, Saitama 351-0198, Japan

ABSTRACT: Amyloid-β (Aβ) peptides represent key players in the pathogenesis of Alzheimer's disease (AD), and mounting evidence indicates that soluble Aβ oligomers mediate the toxicity. Prefoldin (PFD) is a molecular chaperone that prevents aggregation of misfolded proteins. Here we investigated the role of PFD in Aβ aggregation. First, we demonstrated that PFD is expressed in mouse brain by Western blotting and immunohistochemistry and found that PFD is upregulated in AD model APP23 transgenic mice. Then we investigated the effect of recombinant human PFD (hPFD) on Aβ(1−42) aggregation *in vitro* and found that hPFD inhibited Aβ fibrillation and induced formation of soluble Aβ oligomers. Interestingly, cell viability measurements using the 3-(4,5-dimethylthiazol-2-yl)-2,5-diphenyltetrazolium bromide assay showed that Aβ oligomers formed by hPFD were 30−40% less toxic to cultured rat pheochromocytoma (PC12) cells or primary cortical neurons from embryonic C57BL/6CrSlc mice than previously reported Aβ oligomers (formed by archaeal PFD) and Aβ fibrils ($p < 0.001$). Thioflavin T measurements and immunoblotting indicated different structural properties for the different Aβ oligomers. Our findings show a relation between cytotoxicity of Aβ oligomers and structure and suggest a possible protective role of PFD in AD.

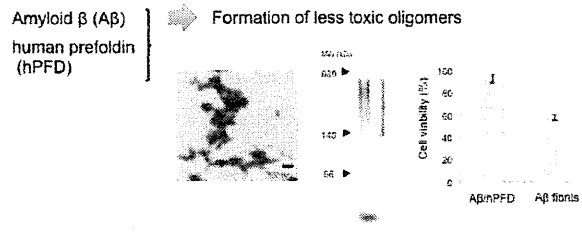

Alzheimer's disease (AD) is pathologically characterized by senile plaques, synapse loss, and accumulation of neurofibrillar tangles in the brain.[1] Senile plaques consist of amyloid-β (Aβ) peptides, which are 40−43 amino acids in length and released from the amyloid precursor protein (APP). Aβ is produced in cultured cells and *in vivo* during normal cell metabolism;[2,3] thus, the presence of Aβ is not a sign of disease itself. Aβ is unstable and aggregates easily once produced. Recent studies have shown a robust correlation between the soluble Aβ oligomer levels and the extent of synaptic loss or severity of cognitive impairment.[4−11] These soluble Aβ oligomers are also toxic to cultured cells.[12,13] By "soluble oligomers", we refer to any dimeric or larger oligomeric structure that is soluble in aqueous solution and remains in solution after high-speed centrifugation.

The structures and sizes of soluble Aβ oligomers vary widely,[14−20] and it remains unclear which oligomeric species represent the toxic form(s). Small, globular Aβ oligomers, termed Aβ-derived diffusible ligands (ADDLs), are reported to play a role in AD pathology.[15,16] However, other constitutions of Aβ are known to be toxic to cells and also to play a role in AD; these include large, spherical structures, termed amylospheroids,[17] and large, spherical Aβ aggregates formed in the presence of liposomes containing GM1 ganglioside.[14] O'Nullain and colleagues recently reported that dimers aggregated rapidly and formed protofibrils that could block long-term potentiation.[19] Takamura et al. found that extracellular and intraneuronal high-molecular weight (HMW) Aβ oligomers caused neuronal degeneration.[18] Hence, several conformations of soluble Aβ oligomers might contribute to neuronal death in AD.

Molecular chaperones represent a diverse group of proteins that recognize and bind unfolded proteins, act to prevent their misfolding and aggregation, and assist their transition to a native conformation.[21−24] The ability of molecular chaperones to prevent off-pathway folding events and to refold proteins that have lost their natural conformation makes them key players in studies of protein misfolding diseases and potential therapeutic agents.[25,26] Indeed, several publications have demonstrated possible roles for molecular chaperones in AD pathology.[27−29] For example, the small heat shock protein αB-crystallin could inhibit Aβ fibrillation and the associated cytotoxicity of Aβ.[27] Cortical neurons expressing Hsp27 were protected against neuronal degeneration caused by Aβ treatment in culture medium,[28] and HspB1 could sequester toxic Aβ oligomers and convert them into large nontoxic aggregates.[29]

Received: December 25, 2012
Revised: April 20, 2013
Published: April 24, 2013

In this study, we investigated the potential role of prefoldin (PFD) in modulating the oligomerization pathway and cytotoxicity of Aβ peptide. PFD is a molecular chaperone conserved in archaea and eukaryotes.[30−32] In the eukaryotic cytosol, it interacts with and stabilizes nascent polypeptides. Eukaryotic PFD is believed to bind to unfolded actins and tubulins and possibly other proteins and to transfer them to cytosolic chaperonin containing TCP-1 (CCT) for folding to the native state.[30,31,33] PFD consists of six subunits, and the subunits can be grouped into two evolutionarily related classes: α and β. Two eukaryotic α-subunits (PFD3 and PFD5) and four β-subunits (PFD1, PFD2, PFD4, and PFD6) exist. Functional PFD hexamers assemble via two β hairpins in the α class subunit and one β hairpin in the β class subunits.[32,34] Both human and archaeal PFD possess quaternary structures resembling a jellyfish with six "tentacles" consisting of coiled coils that interact with and stabilize non-native polypeptides.[34−36]

We previously showed that Aβ fibrillation was inhibited in the presence of archaeal PFD from *Pyrococcus horikoshii* (PhPFD) and that Aβ incubated in the presence of PhPFD formed HMW soluble oligomers that were toxic to cultured rat pheochromocytoma (PC12) cells.[37] In this study, we investigated the potential role of human PFD (hPFD) in modulating Aβ oligomerization and cytotoxicity. First, we confirmed the presence of PFD in mouse brain by immunostaining of brain sections from wild-type (wt) and APP23 transgenic (tg) mice (AD mouse model with 7-fold overexpression of APP and an increasing level of Aβ deposits with age[38]) for PFD. We next investigated hippocampal and cortical brain homogenate of wt and APP23 tg mice and found that PFD was upregulated in APP23 tg mice. Analysis of Aβ and hPFD *in vitro* revealed that Aβ fibrillation was inhibited in the presence of hPFD, as confirmed by Western blot analysis and transmission electron microscopy (TEM). Furthermore, cell viability tests using PC12 cells, or primary cortical neurons, revealed the significantly reduced toxicity of Aβ oligomers that had been incubated with hPFD, in contrast to PhPFD-formed Aβ oligomers.[37] We also demonstrated that nontoxic Aβ oligomers formed by hPFD and toxic Aβ oligomers formed by PhPFD exhibited different antibody recognition properties, as well as different ThT binding properties, which suggests that differences in surface structures might be important for oligomer toxicity.

MATERIALS AND METHODS

Immunohistochemical Studies of PFD Expression in Mouse Brain. Brains from APP23 tg[38] or wt mice were fixed by cardiac perfusion with PBS, incubated overnight in 4% PFA, processed, and embedded in paraffin. Paraffin-embedded 4 μm thick sections were cut and analyzed by immunostaining using goat polyclonal anti-hPFD subunit 5 (hPFD5) (Santa Cruz Biotechnology, Santa Cruz, CA) and secondary anti-goat with tyramide signal amplification (PerkinElmer Life Sciences). The cell nuclei were stained with Hoechst-33342 (Calbiochem, San Diego, CA). As control samples, secondary antibodies with tyramide signal amplifications were added directly to tissues without addition of primary antibodies beforehand (data not shown).

Homogenization of Mouse Brain and Western Blotting. Brains from APP23 tg or wt mice were homogenized with a multibead shocker, metal cone (MC-0214R) at 2500 rpm for 20 s (one cycle) and ultracentrifuged at 70000 rpm for 29 min. Five volumes of homogenization buffer [50 mM Tris-HCl, 150 mM NaCl (pH 7.4), Complete (EDTA plus), and pepstatin A] per brain was used. For Western blotting, three different individuals from either APP23 tg- or wt mice were tested. The homogenate (with protein concentrations normalized to 2 μg/μL) from each individual was mixed with an equal volume of sample buffer and subjected to 15% (w/v) sodium dodecyl sulfate−polyacrylamide gel electrophoresis (SDS−PAGE). The proteins were transferred to a PVDF membrane (Hybond P, GE Healthcare, Little Chalfont, U.K.). After being blocked with 2% ECL Advance blocking agent (GE Healthcare) in 0.1% PBST at 4 °C overnight, the membrane was probed with anti-hPFD5 (1:50) and mouse anti-actin (1:2000) (Sigma, St. Louis, MO). Image J was used to quantify the intensities of the bands. The intensities in wt mice were normalized as 100%.

Expression and Purification of hPFD. The hPFD subunits were expressed in *Escherichia coli* BL21(DE3), purified as described previously,[39] and stored in buffers that included 20% glycerol at −80 °C. Upon being used, the subunits were assembled to a hexameric complex.[39] Briefly, the subunits were combined at equimolar amounts (4−8 nmol) and brought to a final urea concentration of 1.5 M. The mixture was dialyzed against PBS for 1.5 h, fractionated via gel filtration, and analyzed via 15% SDS−PAGE to confirm that the obtained complex included all subunits.

Preparation of Aβ Aggregates. Aβ(1−42) peptide was purchased from Peptide Institute (Osaka, Japan), and seed-free Aβ solutions were prepared as described previously.[14] Briefly, the Aβ peptide was dissolved in a 0.1% ammonia solution at 1.25 mg/mL and ultracentrifuged at 100000 rpm for 3 h to obtain a seed-free Aβ solution.[14] Then the supernatant was collected and stored as aliquots at −80 °C at a concentration of 170 μM (0.77 mg/mL). Before being used, Aβ was thawed, diluted with PBS, and incubated at 25 μM and 37 °C for 48 h, in the absence or presence of various levels of hPFD (1 nM to 5 μM). For a comparison study using archaeal PhPFD, 50 μM Aβ was incubated with 50 μM PhPFD at 50 °C (which is the temperature at which PhPFD is active) for 48 h, which is the appropriate condition for the formation of oligomers as described previously.[37] After incubation, samples were diluted to appropriate concentrations (and equivalent Aβ concentrations for the comparison of Aβ and hPFD vs Aβ and PhPFD) for the following experiments. For Aβ fibril formation, 25 μM Aβ was incubated for 48 h at 37 °C.

Cell Culturing. PC12 cells were cultured in RPMI 1640 medium (Sigma) supplemented with 10% horse serum, 5% fetal bovine serum, 0.1% penicillin, and 0.1% streptomycin on poly-D-lysine (PDL)-coated dishes. For neurite formation, PC12 cells were passaged to PDL-coated dishes to a density of 20000 cells/well and NGF (Invitrogen, Carlsbad, CA) was added to a final concentration of 100 ng/mL. The cells were cultured until they were ready to use as described previously.[14]

Primary cortical neurons were prepared from embryonic C57BL/6CrSlc mice from a developmental state of 16−18 days, according to a previously described method.[40] Briefly, the cells were isolated, washed, and cultured in Neurobasal medium with 2% B27, 0.5 mM glutamine, and penicillin/streptomycin, at a density of 50000 cells/well on poly-L-lysine (PLL)-coated 96-well plates. Primary cortical neurons were cultured for 14 days to allow neurite formation.

Cell Viability Measurements. The viability of PC12 cells and primary cortical neurons was measured using Cell

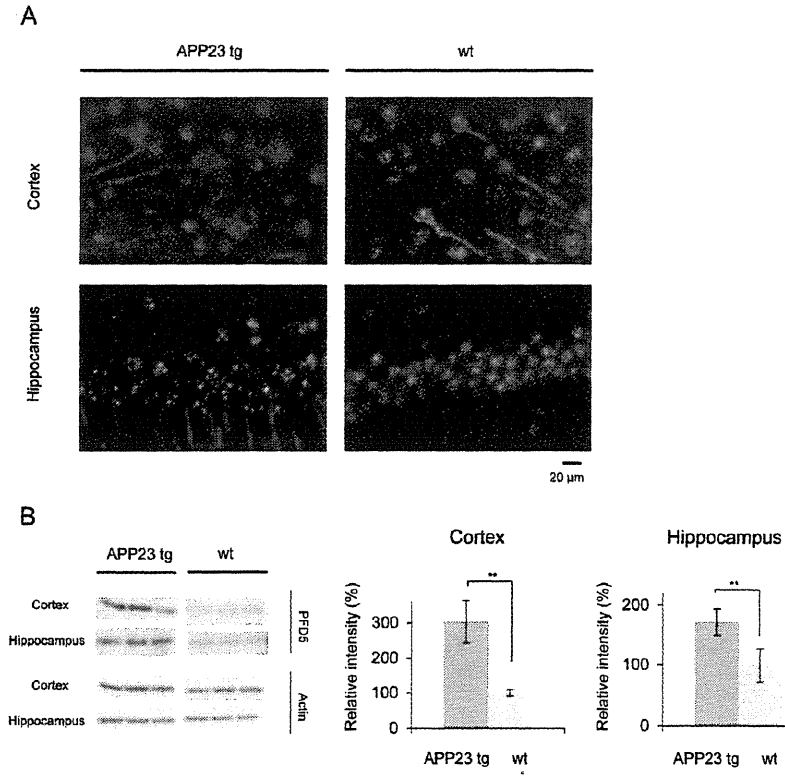

Figure 1. PFD expression in mouse brain. (A) Immunostaining of cortical and hippocampal brain sections from APP23 tg or wt mice with anti-hPFD5: green for PFD and blue for Hoechst. (B) Cortical and hippocampal brain homogenates prepared from APP23 tg or wt mice, analyzed by Western blotting using antibodies for PFD5 (n = 3 per genotype) and actin. Right panels show quantification of the Western blots confirming that expression of PFD is upregulated in APP23 tg mice brain. The intensities in wt mice were normalized as 100%. $^{**}p < 0.01$.

Proliferation Kit I (MTT) from Roche (Indianapolis, IN). PC12 cells (40000 cells/well in 80 μL of medium) were cultured on PDL-coated 96-well plates overnight. Aβ samples (20 μL), aliquoted from the incubated Aβ samples (with and without PFD) and diluted with PBS to the desired Aβ concentrations, were added to the wells and incubated for 16 h for PC12 cells or 24 h for primary cortical neurons. Because 0.5 μM Aβ fibrils exhibited cytotoxicity to PC12 cells (data not shown), the Aβ concentration in the cell culture medium was kept at 0.5 μM unless otherwise stated. For control samples, the same volume of PBS was added to the wells. For the 3-(4,5-dimethylthiazol-2-yl)-2,5-diphenyltetrazolium bromide (MTT) reaction and measurements, the adsorption values at 550 nm were determined using a Tecan (Männedorf, Switzerland) microplate reader. The viability for cells exposed to PBS was used as the 100% viability control.

Native PAGE and Western Blotting. The samples were diluted 1:1 with native PAGE sample buffer, applied to a 5 to 20% gradient Tris-glycine precast gel (Wako, Osaka, Japan), run at a constant current of 10 mA, and then transferred to a nitrocellulose membrane (0.22 μm) (Whatman, Kent, U.K.) at a current of 200 mA for 90 min. The membrane was blocked overnight at 4 °C with 5% skim milk in 0.01% TBST and probed with mouse monoclonal anti-Aβ (6E10, 1:2000, Covance, Princeton, NJ), mouse polyclonal anti-PhPFD[37] (1:2000), or anti-hPFD subunit 3 (hPFD3, 1:1000) (Santa Cruz Biotechnology) antibody, for 1 h at room temperature, followed by secondary horseradish peroxidase-conjugated anti-mouse or anti-goat IgGs (1:2000) (R&D Systems, Minneapolis, MN). Proteins were visualized using the ECL Plus blotting detection reagent (GE Healthcare) according to the manufacturer's instructions. Luminescence was detected in a LAS4000 mini Luminescent Image Analyzer (Fujifilm, Tokyo, Japan), with the Image Reader Las4000 software.

Transmission Electron Microscopy (TEM). One drop of sample was dispensed on a carbon-coated grid and allowed to air-dry. Samarium acetate was used to stain the sample. Samples were observed with an excitation voltage of 80 kV using a JEM-1230 transmission electron microscope (JEOL, Tokyo, Japan).

Immunoprecipitation. Aβ peptide (25 μM, 100 μL) was incubated with 5 μM hPFD. An incubated Aβ sample or hPFD alone samples were used as controls. The samples were diluted to a volume of 1 mL and incubated with 10 μL of anti-Aβ (4G8) overnight at 4 °C while being rotated. The samples were then incubated with 50 μL of Protein G-Sepharose beads (Amersham Biopharma Biotech, Uppsala, Sweden) for 7 h at room temperature. We pulled down all Aβ antibody-bound material with the beads by centrifuging the samples and separating the beads from the supernatant. The immunoprecipitates were washed three times with PBS and thereafter incubated with SDS sample buffer at 95 °C for 5 min. Eluted proteins were loaded on a 15% SDS–PAGE gel and analyzed via Western blotting using anti-hPFD3.

Dot Blot. The dot blot assay was performed as previously described.[41] Samples were incubated at 25 μM Aβ and 5 μM hPFD at 37 °C or at 50 μM Aβ and 50 μM PhPFD at 50 °C. For PFD concentration dependency experiments, 25 μM Aβ was incubated with various concentrations of hPFD (10, 5, 2.5,

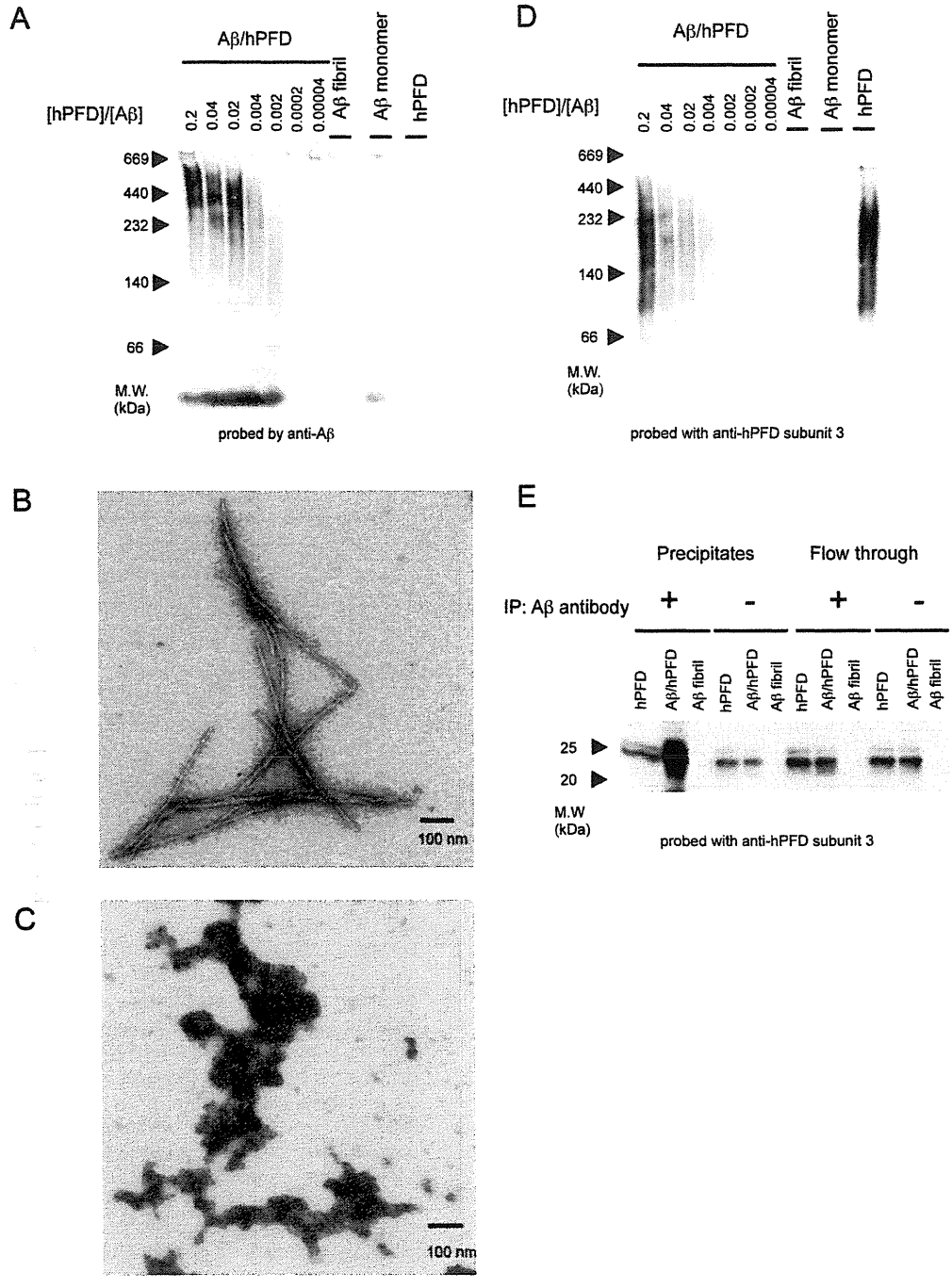

Figure 2. Formation of HMW Aβ oligomers by hPFD. (A) Native PAGE/Western blotting analysis of Aβ aggregates. Aβ samples (25 μM) incubated at 37 °C for 48 h in the absence (Aβ fibril) or presence of varied amounts of hPFD (Aβ/hPFD) were analyzed by native PAGE and probed using mouse monoclonal anti-Aβ (6E10). The ratio of hPFD concentration to Aβ concentration is shown. Unincubated Aβ monomers were used as a control. A HMW native marker kit (GE Healthcare) comprising thyroglobulin (669 kDa), ferritin (440 kDa), catalase (232 kDa), lactate dehydrogenase (140 kDa), and albumin (66 kDa) was used as a molecular weight marker. (B and C) Morphology of insoluble Aβ fibrils formed in the absence of hPFD (B) or soluble Aβ aggregates formed in the presence of hPFD (C) monitored by TEM. The scale bars represents 100 nm. (D) Native PAGE/Western blotting analysis of Aβ samples incubated in the absence (Aβ fibril) or presence of varied amounts of hPFD (Aβ/hPFD) using anti-hPFD3. hPFD was used as a control at a concentration of 5 μM (corresponding to the highest concentration of hPFD incubated with Aβ). The same membrane used in panel A was used and reprobed. (E) Co-immunoprecipitation of hPFD and Aβ. Incubated samples were immunoprecipitated using anti-Aβ (4G8) and Protein G-Sepharose beads. The samples (precipitates and flow through) were then subjected to SDS–PAGE and Western blotting and probed with anti-hPFD3 to confirm interactions between the proteins. As control samples, hPFD alone and Aβ fibril samples were included in the analysis. Samples treated without anti-Aβ were also used as control samples.

0.5, or 0.1 μM) and 50 μM Aβ was incubated with various concentrations of PhPFD (50, 10, 1, 0.2, or 0.01 μM) as described above. The co-incubated Aβ/PhPFD was diluted to an Aβ concentration of 25 μM prior to experiments. ADDL was prepared as described previously.[15] Aβ fibrils and an unincubated Aβ monomer sample were used as controls. The sample mixtures (4 μL) were thereafter spotted onto a nitrocellulose membrane. After being blocked with 5% skim milk and 0.01% TBST for 1 h at room temperature, the membrane was probed with the rabbit polyclonal anti-Aβ oligomer (A11, 1:500) (Biosource, Camarillo, CA), mouse monoclonal anti-Aβ oligomer (4D8, 1:500) (Agrisera, Vännäs, Sweden), or anti-Aβ (6E10, 1:2000) for 1 h at room temperature, followed by washing and probing with secondary antibodies as described above. The 6E10 antibody recognizes amino acid residues 1−16 of Aβ, both monomeric and aggregated forms, whereas 4D8 and A11 antibodies recognize certain Aβ oligomers. ImageJ was used to quantify the intensities of the dots.

ThT and ANS Fluorescence Assays. The structures of Aβ/hPFD and Aβ/PhPFD oligomers were assessed by ANS or ThT fluorescence assay. For ANS fluorescence measurements, Aβ samples (10 μM) were prepared in a PBS buffer containing 50 μM ANS (Sigma). The samples were excited at 370 nm (bandwidth of 10 nm), and the emission spectra were recorded at 470−580 nm. The fluorescence intensity of 50 μM ANS in a PBS solution was used for background subtraction for Aβ fibrils or Aβ monomers, and the fluorescence intensity for binding of ANS to hPFD or PhPFD alone was used as background subtraction for Aβ/hPFD or Aβ/PhPFD. For ThT fluorescence measurements, Aβ samples (5 μM) were prepared in a PBS buffer containing 50 μM ThT (Sigma). The samples were excited at 420 nm (bandwidth of 10 nm), and the emission spectra were recorded at 450−550 nm. The fluorescence intensity of 50 μM ThT in a PBS solution was used for background subtraction for Aβ fibrils or Aβ monomers, and the fluorescence intensity for binding of ThT to hPFD or PhPFD alone was used as background subtraction for Aβ/hPFD or Aβ/PhPFD. All measurements were performed using a Tecan microplate reader. The samples were assayed in triplicate, and the average of the three spectra is presented.

RESULTS

PFD Is Expressed in Mouse Brain. We analyzed brain sections of 6-month-old APP23 tg and wt mice by immunostaining (Figure 1A). Because deposits of Aβ are developed in the cortex and hippocampus of APP23 tg mice,[38] we examined brain sections containing these parts. As shown in the figure, PFD is expressed in the brain in both APP23 tg and wt mice. The expression level of PFD in brains of APP23 tg or wt mice was estimated by analyzing cortical and hippocampal brain homogenate by Western blotting with antibodies directed to PFD subunit 5 (Figure 1B). As shown in the figure, expression of PFD was confirmed in the cortex and hippocampus. Importantly, the level of PFD expression was elevated in both cortex and hippocampus of the APP23 tg mice (Figure 1B), suggesting the possible biological relevance of PFD in AD.

Formation of Soluble Aβ Oligomers in the Presence of hPFD. The effect of hPFD on the aggregation of the Aβ(1−42) peptide was examined *in vitro* with native PAGE and TEM analysis. We previously reported that Aβ fibrillation was inhibited in the presence of archaeal PhPFD.[37] In this work, we examined the fibrillation behavior of Aβ in the presence of hPFD. Figure 2A shows native PAGE/Western blotting analysis of Aβ samples incubated with varied amounts of hPFD. Co-incubation of Aβ and hPFD (Aβ/hPFD) resulted in formation of large soluble Aβ oligomers in a molecular weight distribution between 300 and 600 kDa (Figure 2A), while Aβ incubated in the absence of hPFD under the same conditions did not yield HMW oligomers, indicating that large, insoluble fibrils had been formed that could not enter the gel; these fibrils were confirmed by TEM (Figure 2B). Formation of soluble oligomers was also confirmed with SDS−PAGE/Western blotting analysis (data not shown). Next we investigated the necessary amount of hPFD required to obtain soluble Aβ oligomers and found that an hPFD:Aβ ratio as low as 0.02 (1:50) was sufficient to induce the formation of soluble Aβ oligomers. Even at hPFD:Aβ ratios as low as 0.002 (1:500), soluble Aβ species, including Aβ monomers, were detectable. At lower hPFD concentrations, no soluble Aβ species were observed, which suggests insoluble Aβ fibril formation. These data indicate that substoichiometric amounts of hPFD relative to Aβ are sufficient to observe the antifibrillation phenomenon. The TEM data support the native PAGE/Western blotting data, as large oligomers could be seen in the samples where hPFD was present during incubation (Figure 2C). In soluble Aβ/hPFD, short, prefibrillar structures could also be observed, along with smaller fragments. On the basis of the finding that hPFD inhibited Aβ fibril formation, we studied formation of the complex between hPFD and Aβ by using Western blotting and immunoprecipitation. Figure 2D shows Aβ/hPFD that have been transferred to a nitrocellulose membrane and probed with anti-hPFD, derived from a native gel used in Figure 2A. hPFD alone appeared on the gel within the molecular weight range of ~100−400 kDa. Co-incubated Aβ/hPFD gave an hPFD signal within the molecular weight range of ~100−500 kDa with main protein fractions found between 200 and 300 kDa. Because most of the Aβ was detected in the molecular weight range of 300−500 kDa (Figure 2A), most of the hPFD is most likely not in complex with the Aβ oligomers.

To further examine the possible formation of a complex, co-incubated Aβ/hPFD were immunoprecipitated using anti-Aβ (4G8) and Protein G-Sepharose beads and detected by Western blotting using anti-hPFD (Figure 2E). As shown in the figure, a significant amount of hPFD could be detected in the precipitate, supporting a direct interaction between hPFD and Aβ. For the control experiments, the samples were precipitated in the absence of anti-Aβ. The faint bands observed in the control experiments are likely to be due to unspecific binding of hPFD to the Sepharose beads (however, not to anti-Aβ, because the intensity of the band of hPFD incubated with anti-Aβ was similar to the intensity of the band of hPFD incubated without anti-Aβ). Taken together, although these results propose a direct interaction between hPFD and Aβ for oligomer formation, the binding is likely to be transient and/or weak.

Toxicity of Aβ/hPFD Oligomers to PC12 and Primary Neuron Cells. Accumulated evidence has suggested that soluble Aβ oligomers are toxic to neurons in AD brains.[4−9,11,37] To investigate the cytotoxicity of the Aβ oligomers, we added Aβ oligomers to cultured rat pheochromocytoma PC12 cells, or primary neurons. The cytotoxicity of the Aβ oligomers formed in the presence of hPFD to PC12 cells is shown in Figure 3A. Intriguingly, the Aβ oligomers formed in the presence of hPFD resulted in a cell viability higher than that for Aβ fibrils alone.

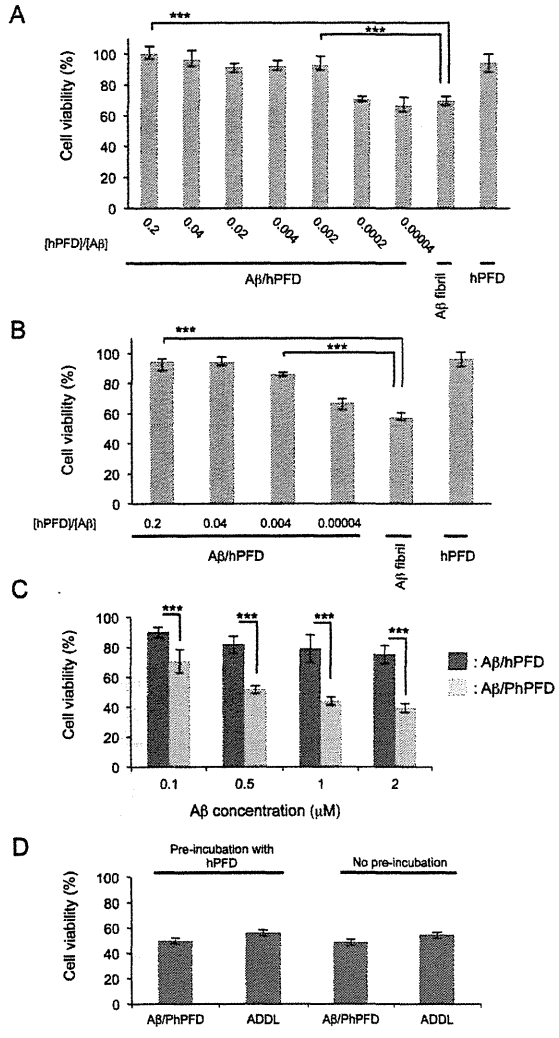

Figure 3. Reduced cytotoxicity of Aβ oligomers formed by hPFD. (A and B) Cytotoxicity assays of Aβ oligomers formed in the presence of hPFD with PC12 cells (A) and differentiated PC12 cells with NGF (B) using the MTT assay. The ratio of hPFD concentration to Aβ concentration (25 μM) during incubation is shown. The Aβ concentration in the cell culture medium was 0.5 μM. Aβ fibrils and hPFD were used as control samples. Data are shown as means ± the standard deviation (SD) of three experiments. ***$p < 0.001$. (C) Cytotoxicity assays of Aβ oligomers formed with hPFD (Aβ/hPFD) or PhPFD (Aβ/PhPFD) samples against primary cortical neurons using the MTT assay. The Aβ samples were incubated with the cells for 24 h at the indicated concentrations prior to viability measurements. ***$p < 0.001$. (D) Viability of PC12 cells exposed to toxic Aβ oligomers after preincubation with hPFD. hPFD (1 μM) was added to the cell medium 4 h prior to the addition of 0.5 μM toxic Aβ oligomers (Aβ/PhPFD or ADDL).

To investigate the concentration of hPFD needed to inhibit Aβ cytotoxicity, we compared the toxicity of samples incubated at various hPFD concentrations (Figure 3A). We observed that a molar concentration of hPFD as much as 500-fold lower than the concentration of Aβ ([hPFD]/[Aβ] = 0.002) significantly reduced the cytotoxicity. The ratios of hPFD to Aβ that reduce cytotoxicity are similar to those that prevented *in vitro* fibrillation (Figure 2A). It should be noted that the cell toxicity was similar for NGF differentiated PC12 cells (Figure 3B). However, the reduced toxicity was unexpected because our previous study showed that Aβ oligomers formed by co-incubation of Aβ and archaeal PhPFD (Aβ/PhPFD) were more cytotoxic than Aβ fibrils.[37] Thus, we also examined the cytotoxicity of the Aβ oligomers using primary neurons, by comparing the viability of cells that had been exposed to either Aβ/hPFD or Aβ/PhPFD at different concentrations (Figure 3C). As shown in the figure, primary neurons exposed to hPFD-formed Aβ oligomers were significantly more viable than cells exposed to PhPFD-formed Aβ oligomers.

We then addressed whether the reduced toxicity of the Aβ oligomers formed in the presence of hPFD could be due to the ability of hPFD itself to protect the cells against cell death. To examine this, we preincubated PC12 cells with 1 μM hPFD for 4 h, before addition of 0.5 μM toxic Aβ oligomers (ADDL or Aβ/PhPFD), followed by viability measurements with the MTT assay (Figure 3D). Our results show clearly that the cytotoxicity was preserved, even with hPFD in the solution, which indicates that hPFD itself does not prevent the toxic effect of preformed toxic oligomers.

Difference between Aβ Oligomers Formed by hPFD and PhPFD. Our study revealed differences in cytotoxicity between Aβ oligomers formed by eukaryotic hPFD and archaeal PhPFD. To compare these Aβ oligomers of different toxicities, co-incubated Aβ/hPFD or Aβ/PhPFD were subjected to native PAGE followed by Western blotting using anti-Aβ (Figure 4A). Incubation temperatures and concentrations appropriate for obtaining effective Aβ oligomerization in the presence of each chaperone were applied. Formed Aβ oligomers appeared to be of similar size (HMW soluble oligomers within the molecular weight range of 200–500 kDa) regardless of which chaperone we used (Figure 4A). Then we hypothesized that the HMW Aβ oligomers formed by co-incubation with hPFD or PhPFD might differ in shape and/or surface structure with different parts of the Aβ sequence exposed, leading to different toxic properties. Comparing TEM data of the Aβ/hPFD oligomers (Figure 2C) and the Aβ/PhPFD oligomers,[37] we could not observe significant differences between the oligomers, which both consisted of large oligomers and prefibrillar aggregates. To further investigate possible differences in structures, we examined the antibody recognition properties of the Aβ oligomers using various anti-Aβ antibodies. The hPFD- or PhPFD-formed Aβ oligomer samples were spotted on nitrocellulose membranes and probed with 6E10, 4D8, or A11 antibodies, and the intensities of the signals were compared (Figure 4B). We obtained different intensities of signals for the different antibodies reacting with the same concentration of different Aβ oligomeric species, Aβ monomers, or Aβ fibrils. The 4D8 antibody bound more strongly to Aβ/PhPFD than Aβ/hPFD. On the other hand, the binding of A11 to Aβ/hPFD was stronger than that to Aβ/PhPFD (Figure 4B). The intensity of the Aβ/PhPFD dot was approximately 60% of the intensity of the Aβ/hPFD dot for the A11 antibody. To further confirm the difference in antibody recognition, Aβ/hPFD and Aβ/PhPFD incubated at various concentrations of hPFD or PhPFD were prepared and analyzed with a dot blot assay using the A11 antibody (Figure 4C). As shown in the figure, the antibody signal intensities increased in a dose-dependent manner when Aβ was incubated with PFDs at higher concentrations, and the A11 antibody showed stronger affinity for Aβ/hPFD than for Aβ/PhPFD at different

dx.doi.org/10.1021/bi301705c | *Biochemistry* 2013, 52, 3532–3542

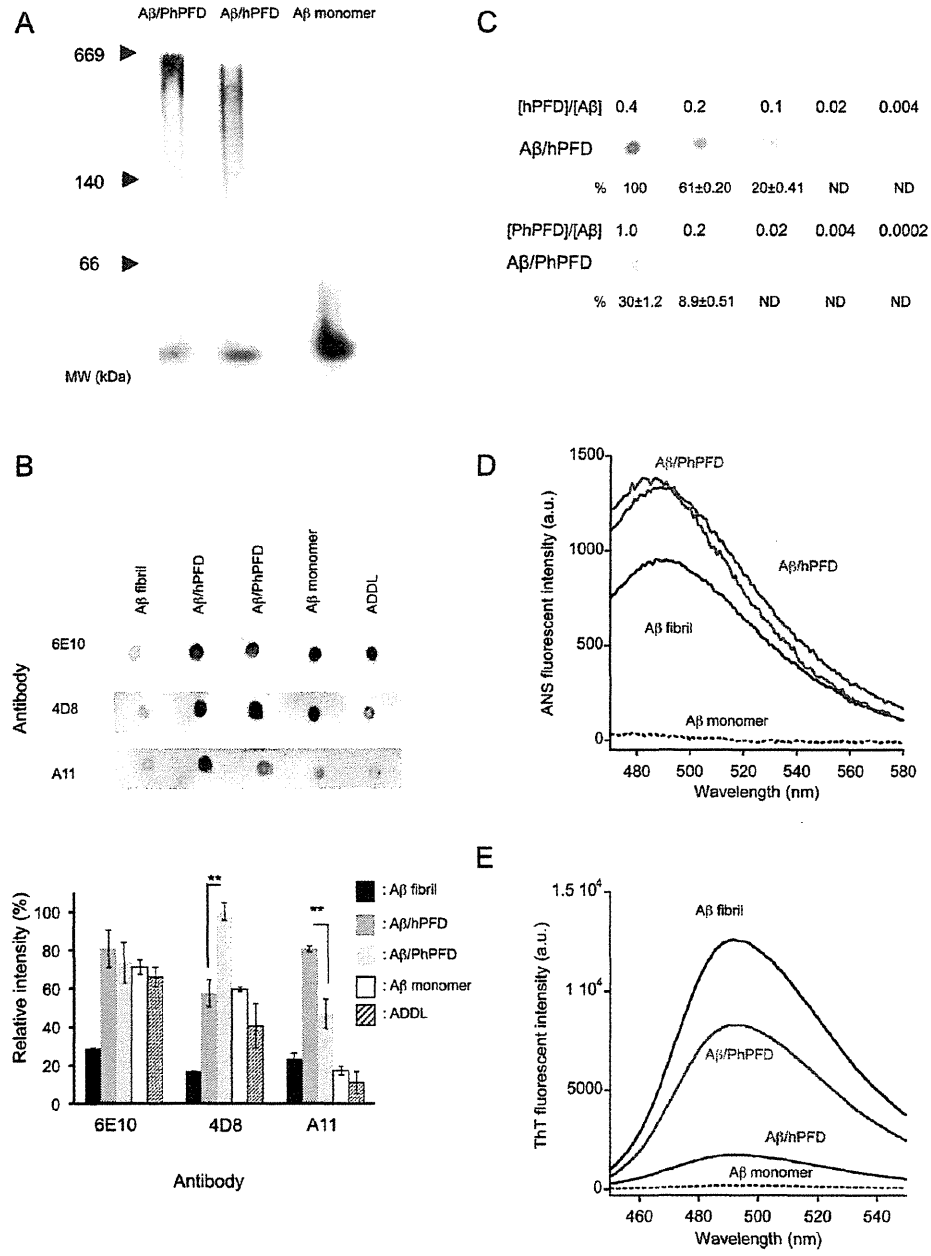

Figure 4. Comparison between Aβ oligomers formed by hPFD and PhPFD. (A) Native PAGE/Western blotting analysis of Aβ oligomers formed in the presence of PhPFD (Aβ/PhPFD) and hPFD (Aβ/hPFD). Incubated samples were analyzed by native PAGE and probed using mouse monoclonal anti-Aβ (6E10). The Aβ monomer was used as a control. (B) Dot blot assay of Aβ oligomers formed in the presence of hPFD (Aβ/hPFD) or PhPFD (Aβ/hPFD) using various Aβ antibodies as indicated. Aβ fibril, Aβ monomer, or ADDL was used for comparison. Samples were spotted onto nitrocellulose membranes and probed with the 6E10, 4D8, or A11 anti-Aβ antibody. The intensity of each spot was quantified with ImageJ and compared, confirming the different affinities of the different Aβ oligomers for the different antibodies. The intensity in Aβ/PhPFD with the 4D8 antibody was normalized as 100%. Data are shown as means ± SD of two spots. $^{**}p < 0.01$. (C) Dot blot of Aβ oligomers formed in the presence of various concentrations of hPFD or PhPFD. Samples were spotted onto a nitrocellulose membrane probed with the A11 antibody. ImageJ was used for quantification. The intensity in Aβ/hPFD ([hPFD]/[Aβ] = 0.4) was normalized as 100%. Data are shown as means ± SD of two spots. (D) ANS fluorescence spectra comparing the Aβ fibril (black), Aβ/PhPFD (blue), Aβ/hPFD (red), and Aβ monomer (dotted). Samples were prepared in triplicate at 10 μM Aβ and 50 μM ANS in a volume of 100 μL. ANS fluorescence with hPFD or PhPFD alone was used as a background and subtracted from the Aβ/hPFD or Aβ/PhPFD, respectively. The samples were excited at 370 nm. Emission was measured from 470 to 580 nm. (E) ThT fluorescence spectra comparing the Aβ fibril (black), Aβ/PhPFD (blue), Aβ/hPFD (red), and Aβ monomer (dotted). Samples were prepared in triplicate at 5 μM Aβ and 50 μM ThT in a volume of 100 μL. As described above, the ThT fluorescence with hPFD or PhPFD alone was used as background subtraction for Aβ/hPFD or Aβ/PhPFD. The samples were excited at 420 nm. Emission was measured from 450 to 550 nm.

concentrations, which also supports different antibody recognition properties between these two oligomers.

The structural properties of Aβ/hPFD and Aβ/PhPFD oligomers were further examined by the hydrophobicity probe, ANS, and the amyloid probe, thioflavin T (ThT). As shown in Figure 4D, binding of ANS to Aβ/hPFD or Aβ/PhPFD was similar, which indicates that the surface hydrophobicity of the compared Aβ oligomers is similar. On the contrary, in the case of ThT binding, a significant difference in ThT binding was observed between Aβ oligomers formed in the presence of either hPFD or PhPFD (Figure 4E). It was previously shown that Aβ/PhPFD gave a weaker ThT fluorescent signal than Aβ fibrils.[37] Here, we compared the ThT binding properties for Aβ/PhPFD and Aβ/hPFD and found that Aβ/hPFD gave an even weaker ThT fluorescent signal than Aβ/PhPFD, which suggests that the amount of accumulated β-sheets of Aβ/hPFD is smaller than of Aβ/PhPFD, or that the β-sheet stacking manner is different. Taken together, these data suggest that difference in toxicity between Aβ oligomers formed by human and archaeal PFD might be correlated with differences in protein conformation, such as exposed amino acid residues, geometrical features, and β-sheet packing.

DISCUSSION

Soluble oligomers of Aβ are considered toxic species that contribute to AD pathology.[4−11] For example, Aβ oligomers can block hippocampal long-term potentiation *in vivo*[42] and trigger synaptic loss leading to cognitive impairment.[43] The structures and sizes of soluble Aβ oligomers vary widely, and which oligomeric species represents the toxic form(s) remains unclear. Protein misfolding and aggregation are very complex processes; aside from the size of Aβ oligomers potentially correlating with its toxic properties, the surface structure, shape, and composition of the oligomers likely represent important parameters of toxicity. The Aβ aggregation pathway might also be of importance for its toxicity, and environmental factors such as chaperones or other components of the cellular homeostasis machinery might play important roles in this pathway.[11,26,44,45]

Molecular chaperones are known to prevent protein aggregation and to function to protect against toxicity of misfolded proteins.[26,44−46] There are studies describing how molecular chaperones can prevent toxicity of Aβ, or other proteins that are toxic to cells.[27,47−51] However, there are also contradictory reports suggesting that chaperones might trap the growing amyloids in a toxic state.[37,52,53]

In this study, we confirmed the presence of PFD in the cortex and hippocampus of APP23 tg or wt mice, the same regions of the brain that are strongly affected in AD. We also investigated the effect of hPFD on Aβ aggregation using recombinant hPFD and demonstrated for the first time that Aβ fibrillation was inhibited in the presence of hPFD and large, soluble oligomers were formed. Even at substoichiometric hPFD:Aβ ratios down to 1:500, hPFD had an effect on Aβ fibrillation (Figure 2A). One of the important cellular roles of a molecular chaperone is to bind and release its substrate in a repetitive cycle, until the target protein has been correctly folded,[22,24,54] potentially explaining how comparatively low levels of chaperone complexes can affect the folding of a molar excess of a target substrate. This is also consistent with our results suggesting that the interaction between hPFD and Aβ is likely to be transient and/or weak (Figure 2).

Importantly, we found that Aβ oligomers formed in the presence of hPFD were less toxic to cultured cells and primary neurons, which contradicts our previous finding of toxic Aβ oligomers formed in the presence of archaeal PhPFD.[37] The sizes of these oligomers appeared to be similar at least by native gel analysis. However, we found that both antibody recognition and ThT binding were different, which suggests that there are differences in the molecular surfaces and conformations of these oligomers. Previous studies have shown that the substrate binding mechanism differs between eukaryotic and archaeal PFD.[34,35] Thus, it is plausible that different substrate binding between hPFD and PhPFD might lead to differences in the modulation of oligomerization, and ultimately different physical and chemical attributes of the surface structure.

It has been shown that the structures of Aβ oligomers are related to their toxic properties. Takamura et al. reported that recognition of Aβ HMW oligomers with newly generated monoclonal antibodies could be correlated with their toxicity.[18] In a recent paper by Sinha et al., the authors reported that lysine specific molecular compounds inhibited fibrillation of amyloidogenic proteins and induced nontoxic oligomer formation.[55] These nontoxic oligomers had a lower affinity for the A11 antibody than toxic oligomers. In another study, the A11 antibody was found to recognize soluble oligomers of various proteins.[41,56] It was also shown that the two oligomers with different toxicities showed differences in their recognition by Aβ antibodies.[57] In another study by Noguchi et al., toxic oligomers were not recognized by A11 oligomers, but by another oligomer specific antibody.[58] These studies suggest that antibody recognition of Aβ oligomers is related to their toxic properties, which is consistent with our results. Previous studies showed that oligomer toxicity could be mediated via cell surface receptors.[11,59,60] Thus, it is plausible that receptor recognition could be different between the PhPFD- and hPFD-formed oligomers. Another hypothesis is that the interactions between the oligomers and the cell membranes are crucial for the toxicity, and that toxic oligomers can disturb the monolayers in the cell membrane and cause cell death.[61] Thus, it is also plausible that interactions with cell membranes might be different between PhPFD- and hPFD-formed oligomers.

Our results using structural probes such as ANS and ThT strengthen the idea that different structures of protein aggregates decide their toxic properties. ANS is a molecule that recognizes hydrophobic sites in proteins. Studying the binding affinity of ANS for different protein structures therefore gives a hint about the amount of exposed hydrophobic sites in the structures. We did not obtain significantly different ANS fluorescence results while comparing Aβ/hPFD and Aβ/PhPFD, which indicates that the surface hydrophobicities of the different oligomers are similar. Interestingly, however, the ThT fluorescence values showed a clear difference. ThT is believed to recognize and bind to the "cross β structure", which is a common motif in protein fibrils and aggregates.[62] Therefore, our data show that the less toxic Aβ oligomer might contain fewer cross β motifs. It was recently described that toxic fibrillar oligomers of Aβ are rich in cross β structure,[63] which is consistent with our ThT binding and toxicity data. When these studies are put together, it is plausible that the inner and outer structure of Aβ oligomers might be crucial in Aβ-mediated toxicity, such as the composition of exposed amino acid residues and protein packing.

PFD is known as a cytosolic protein, with a crucial function in protein folding.[22] However, it might be found in the extracellular space. It has been shown that tau and other intracellular components can be found in the extracellular space

upon neuron death, and subsequently in the cerebrospinal fluid, for example, in AD.[64−66] Thus, it is possible that PFD also could be released into the extracellular space. In addition, it has recently become obvious that Aβ is produced intracellularly (see review 9, for example). Recent findings also support the idea that Aβ is present within the cytosolic compartment. For example, intracellular accumulation of Aβ is linked to cytosolic proteasome inhibition, and proteasome inhibition leads to higher Aβ levels.[67−69] In this study, we have shown that PFD is expressed in cortical neurons and is upregulated in APP23 tg mice, supporting a putative connection of hPFD to AD *in vivo*. This is consistent with a recent genomewide expression study of AD patients, which showed that PFD and CCT genes are upregulated in AD.[70,71] Thus, it is possible that hPFD could modulate the folded state of a subpopulation of intracellular Aβ to exert protective effects on cells.

The data presented in this work provide the first description of a potential molecular basis for hPFD in modulating Aβ aggregation. Our findings also contribute to the understanding of the diversity of Aβ oligomerization and its subsequent toxicity and will stimulate other studies involving the relationship between molecular chaperones and their influence on protein misfolding disorders such as AD.

AUTHOR INFORMATION

Corresponding Author

*Bioengineering Laboratory, RIKEN, 2-1 Hirosawa, Wako, Saitama 351-0198, Japan. Telephone: +81-48-967-9312. Fax: +81-48-462-4658. E-mail: zako@riken.jp (T.Z.) or mizuo@riken.jp (M.M.).

Present Address

‖P.C.S.: Michael Smith Laboratories, University of British Columbia, 2185 East Mall, Vancouver, BC V6T 1Z4, Canada.

Funding

We are grateful for financial support from RIKEN (K.M.S., T.Z., and M.M.), the Ministry of Education, Science, Sports, Culture and Technology of Japan (MEXT) (T.Z. and M.M.), and the Canadian Institutes of Health Research (CIHR; Grant MOP-84523 to M.R.L.). K.M.S. is a Foreign Postdoctoral Researcher of RIKEN. P.C.S. acknowledges scholarships from the Natural Sciences and Engineering Research Council of Canada (NSERC) and the Michael Smith Foundation for Health Research (MSFHR). M.R.L. is the recipient of a senior scholar award from the MSFHR.

Notes

The authors declare no competing financial interest.

ABBREVIATIONS

AD, Alzheimer's disease; Aβ, amyloid-β; ADDLs, Aβ-derived diffusible ligands; PFD, prefoldin; CCT, cytosolic chaperonin containing TCP-1; PhPFD, PFD from *P. horikoshii*; TEM, transmission electron microscopy; Aβ/hPFD, Aβ sample(s) incubated with hPFD; Aβ/PhPFD, Aβ sample(s) incubated with PhPFD; ThT, thioflavin T.

REFERENCES

(1) Selkoe, D. J. (2004) Cell biology of protein misfolding: The examples of Alzheimer's and Parkinson's diseases. *Nat. Cell Biol. 6*, 1054−1061.

(2) Shoji, M., Golde, T. E., Ghiso, J., Cheung, T. T., Estus, S., Shaffer, L. M., Cai, X. D., McKay, D. M., Tintner, R., Frangione, B., et al. (1992) Production of the Alzheimer amyloid β protein by normal proteolytic processing. *Science 258*, 126−129.

(3) Selkoe, D. J. (1998) The cell biology of β-amyloid precursor protein and presenilin in Alzheimer's disease. *Trends Cell Biol. 8*, 447−453.

(4) Caughey, B., and Lansbury, P. T. (2003) Protofibrils, pores, fibrils, and neurodegeneration: Separating the responsible protein aggregates from the innocent bystanders. *Annu. Rev. Neurosci. 26*, 267−298.

(5) Chiti, F., and Dobson, C. M. (2006) Protein misfolding, functional amyloid, and human disease. *Annu. Rev. Biochem. 75*, 333−366.

(6) Ferreira, S. T., Vieira, M. N., and De Felice, F. G. (2007) Soluble protein oligomers as emerging toxins in Alzheimer's and other amyloid diseases. *IUBMB Life 59*, 332−345.

(7) Glabe, C. G. (2008) Structural classification of toxic amyloid oligomers. *J. Biol. Chem. 283*, 29639−29643.

(8) Haass, C., and Selkoe, D. J. (2007) Soluble protein oligomers in neurodegeneration: Lessons from the Alzheimer's amyloid β-peptide. *Nat. Rev. Mol. Cell Biol. 8*, 101−112.

(9) Laferla, F. M., Green, K. N., and Oddo, S. (2007) Intracellular amyloid-β in Alzheimer's disease. *Nat. Rev. Neurosci. 8*, 499−509.

(10) Roychaudhuri, R., Yang, M., Hoshi, M. M., and Teplow, D. B. (2009) Amyloid β-protein assembly and Alzheimer disease. *J. Biol. Chem. 284*, 4749−4753.

(11) Sakono, M., and Zako, T. (2010) Amyloid oligomers: Formation and toxicity of Aβ oligomers. *FEBS J. 277*, 1348−1358.

(12) Hartley, D. M., Walsh, D. M., Ye, C. P., Diehl, T., Vasquez, S., Vassilev, P. M., Teplow, D. B., and Selkoe, D. J. (1999) Protofibrillar intermediates of amyloid β-protein induce acute electrophysiological changes and progressive neurotoxicity in cortical neurons. *J. Neurosci. 19*, 8876−8884.

(13) Chromy, B. A., Nowak, R. J., Lambert, M. P., Viola, K. L., Chang, L., Velasco, P. T., Jones, B. W., Fernandez, S. J., Lacor, P. N., Horowitz, P., Finch, C. E., Krafft, G. A., and Klein, W. L. (2003) Self-assembly of Aβ(1−42) into globular neurotoxins. *Biochemistry 42*, 12749−12760.

(14) Yamamoto, N., Matsubara, E., Maeda, S., Minagawa, H., Takashima, A., Maruyama, W., Michikawa, M., and Yanagisawa, K. (2007) A ganglioside-induced toxic soluble Aβ assembly. Its enhanced formation from Aβ bearing the Arctic mutation. *J. Biol. Chem. 282*, 2646−2655.

(15) Lambert, M. P., Barlow, A. K., Chromy, B. A., Edwards, C., Freed, R., Liosatos, M., Morgan, T. E., Rozovsky, I., Trommer, B., Viola, K. L., Wals, P., Zhang, C., Finch, C. E., Krafft, G. A., and Klein, W. L. (1998) Diffusible, nonfibrillar ligands derived from Aβ1−42 are potent central nervous system neurotoxins. *Proc. Natl. Acad. Sci. U.S.A. 95*, 6448−6453.

(16) Klein, W. L. (2002) Aβ toxicity in Alzheimer's disease: Globular oligomers (ADDLs) as new vaccine and drug targets. *Neurochem. Int. 41*, 345−352.

(17) Hoshi, M., Sato, M., Matsumoto, S., Noguchi, A., Yasutake, K., Yoshida, N., and Sato, K. (2003) Spherical aggregates of β-amyloid (amylospheroid) show high neurotoxicity and activate tau protein kinase I/glycogen synthase kinase-3β. *Proc. Natl. Acad. Sci. U.S.A. 100*, 6370−6375.

(18) Takamura, A., Okamoto, Y., Kawarabayashi, T., Yokoseki, T., Shibata, M., Mouri, A., Nabeshima, T., Sun, H., Abe, K., Urisu, T., Yamamoto, N., Shoji, M., Yanagisawa, K., Michikawa, M., and Matsubara, E. (2011) Extracellular and intraneuronal HMW-AβOs represent a molecular basis of memory loss in Alzheimer's disease model mouse. *Mol. Neurodegener. 6*, 20.

(19) O'Nullain, B., et al. (2010) Amyloid β-Protein Dimers Rapidly Form Stable Synaptotoxic Protofibrils. *J. Neurosci.*, 14411−14419.

(20) Uversky, V. N. (2010) Mysterious oligomerization of the amyloidogenic proteins. *FEBS J. 277*, 2940−2953.

(21) Bukau, B., Weissman, J., and Horwich, A. (2006) Molecular chaperones and protein quality control. *Cell 125*, 443−451.